STUDY OF STRUCTURAL AND ELECTRONIC PROPERTIES OF TRANSITION METAL IRON AND NICKEL

A Dissertation

Submitted for the Partial Fulfillment of

Requirements for the Masters of Science Degree in Physics

Bishnu Dhakal

T.U. Registration No: 5-2-19-2071-2009

Symbol No: Phy. 1305/072

DEPARTMENT OF PHYSICS

INSTITUTE OF SCIENCE AND TECHNOLOGY

BIRENDRA MULTIPLE CAMPUS,

BHARATPUR CHITWAN

October, 2020

DECLARATION

I, "Bishnu Dhakal", hereby declare that the work presented here is genuine work done originally by me and has not been published or submitted elsewhere for the requirement of a degree program. Any literature, data or works done by others and cited in this dissertation has been given due acknowledgement and listed in the reference.

_____

Bishnu Dhakal

Date:

RECOMMENDATION LETTER

This is to certify that the dissertation work entitled **"STUDY OF STRUCTURAL AND ELECTRONIC PROPERTIES OF TRANSITION METAL IRON AND NICKEL**" has been carried out by **Mr. Bishnu Dhakal** as the partial fulfillment for the requirement of M.Sc. Degree in Physics under our supervision. To the best of my knowledge, this work is original and is not been submitted to any other degree in this institute.

……..	……..
Supervisor	Supervisor
Prof. Dr. Sitaram Bahadur Thapa	Dr. Rajendra Prasad Adhikari
Department of Physics	Department of Natural Science
Birendra Multiple Campus	(Applied Physics)
Tribhuvan University	Kathmandu University
Bharatpur, Nepal	Dhulikhel, Kavre
Date…….	Date…….

ABSTRACT

We optimize lattice parameter and identify the nature and values of band gap of iron and nickel using quantum espresso and Pseudo-Potential density functional Theorem. During optimization, the kinetic energy cut-off energy is found to be 95 Ry for Fe having k-point grid (8×8×8) for Fe. Then we estimate the lattice Parameter is found to be 5.42 Bohr for Fe which is very near with experimental results as well as previous calculated data. Which is only 0.05% deviated from experimental result and previous data. The kinetic energy cut-off energy is found to be 95 Ry for having k-point grid (6×6×6) for Ni. Then we estimate the lattice Parameter is found to be 6.66 Bohr for Ni which is very near with experimental results as well as previous calculated data. Which is only 0.015% deviated from experimental result and previous data. Thus the lattice parameter of Fe and Ni estimated with GGA method is in close agreement with experimental values. Then we have study the band structure and found bands are overlap, density of states and partial density of states is very smooth and p-orbital have very less contribution in PDOS using GGA method in QE package.

ACKNOWLEDGEMENTS

During the study and completion of this Dissertation I have benefited from many peoples to whom I would like to express my sincere thanks.

In this insightful delight I would first of all convey my sincere gratefulness to my supervisors **Prof. Dr. Sitaram Bahadur Thapa** and **Dr. Rajendra P. Adhikari** for providing me intellectual suggestions and very useful guidance without whose companionship of my thesis would ever have come to this stage.

Also, I am equally thankful to The **former campus chief Mr. Govinda Sapkota, campus chief Prof. Dayaram Poudel, Head of the Department Prof. Arun Kumar Shrestha.** I also express my sincere thanks to Prof. Dr. Harihar poudyal, Associate Prof. Dilli Prasad Sapkota, Dr. Seshkant Adhikari, Mr. Ekraj Poudel, Mr. Rajendra Neupane, Mr. Uday Bahadur Thapa, Mr. Ram Krishna Tiwari, Mr. Sanjay Shah, Mr. Rabindra Raj Bista, Mr. Madan Phuyal, Mr. Moti Bhusal, Mr. Ishwor Chandra Poudel, Mr. Pratap Koirala Mr. Rudra Poudel and all the respected faculty members of Physics Department of Birendra Multiple Campus.

The acknowledgement would be incomplete if I don't mention my friends Mr. Dhruba Sapkota, Mr. Amrit Sharma, Mr. Shiva Prasad Bhusal and Mr. Suresh Ghimire for their consistent help and warm support during this work.

I would like to remember my family, their support and encouragement. This work would not have been possible without the love and patience of my family. So, I want to give huge respect to my father Mr. Ram Parsad Dhakal, mother Mrs. Shiva Kanti Dhakal, my wife Mrs Pooja Dhakal and my sisters. I am also thankful to all my friends , relatives and well wishers for their valuable support and suggestions during this project.

It is impossible to remember all to whom I owe my gratitude, and I apologize to those I've inadvertently left out.

Bishnu Dhakal

TABLE OF CONTENTS

Contents ..... Page

TITLE PAGE i

DECLARATION ii

RECOMMENDATION LETTER iii

EVALUATION iv

ABSTRACT v

ACKNOWLEDGEMENTS vi

TABLE OF CONTENTS vii

LIST OF TABLES ix

LIST OF FIGURES x

LIST OF ABBREVIATIONS xii

CHAPTER 1 : INTRODUCTION 1

1.1 General Consideration 1

1.2 Study Material: Iron and Nickel 13

1.2.1 Crystal Structure 14

1.2.2 Scope of the Present Work 16

1.3 How we Approach? 17

CHAPTER 2 : LITERATURE REVIEW OF IRON AND NICKEL 18

CHAPTER 3 : THEORY 20

3.1 General consideration 20

3.2 Born-Oppenheimer approximation 20

3.3 Hartree-Fock Approximation 24

3.4 Density functional theory 26

3.5 The Kohn-Sham approach 27

3.6 The Local Density Approximation 29

3.7 The Generalized Gradient approximation 30

3.8 Pseudo-potentials 32

3.9 Band Structure 35

3.10 GW approximation 36

CHAPTER 4 : METHODOLOGY 38

4.1 General Consideration 38

4.2 Quantum Espresso Program 38

4.2.1 PWscf 40
4.2.2 Post Processing 41
CHAPTER 5: RESULTS AND CONSIDERATION 42
5.1 General Consideration 42
5.2 Structural Optimization: 42
5.2.1 Kinetic Energy cut-off (ecutwfc) 43
5.2.2 Lattice Parameter 45
5.2.3 k-point grid 47
5.2.4 Degauss 49
5.3 Band structure 50
5.4 Density of States 52
5.5 Partial Density of States 54
CHAPTER 6 : CONCLUSION AND CONCLUDING REMARKS: 56
6.1 Further Enhancement 57
BIBLIOGRAPHY 58
APPENDIX 62

LIST OF TABLES

TABLE **PAGE**

1.1 Different types of lattice system 9

1.2 Characteristics of cubic lattices 10

1.3 Introduction of Fe and Ni..... 16

LIST OF FIGURES

TABLE		PAGE
1.1	Two lattice points P_1 and P_2 of a three-dimensional lattice connected by translation vector t	4
1.2	Crystal structure	4
1.3	The construction of Wigner-Seitz cell for a two-dimensional space lattice	5
1.4	Miller indices of lattice planes: (a, b) (100); (c, d) (010); (e, f) (001), (g, h) (110); (i) (111)	6
1.5	Part of the set of (122) lattice planes Bravais lattice in two dimensions	6
1.6	Bravais lattice in 2D. The five conceivable Bravais lattices in 2D are depicted from (a) to (e)	7
1.7	Brillouin zone	12
1.8	When a particle is enclosed in cubical box of dimension L the energy levels are discrete	13
1.9	Crystal structure of bcc, fcc and hcp phase	15
3.1	Typical molecular potential for the nuclei in the molecule. Ro characterizes the relative equilibrium position of the two nuclei. R represents the relative nuclear distance	23
3.2	Schematic representation of iterative solution of coupled single-particle equations. This kind of operation is easily implemented on the computer	25
3.3	2p radial wave functionψr for oxygen treated in the LDA, comparing the all-electron function (solid line), a pseudofunction generated using the Hamann approach (dotted line), and the smooth part of the pseudofunctionψ in the "ultrasoft" method (dashed line)	33
3.4	Figurative illustration of a semiconductor band structure, plotted along one crystal direction. The upper “band” (line) will be essentially empty of electrons, and is called the conduction band; the lower band will be essentially full of electrons, and is called the valence band	36
5.1	The plot of Total energy with cut-off energy of Fe	44
5.2	The plot of Total energy with cut-off energy of Ni	45
5.3	The plot of Total energy with lattice parameter of Fe	46
5.4	The plot of Total energy with lattice parameter of Ni	47

5.5 The plot of Total energy with k-point grid of Fe 48
5.6 The plot Total energy with k-point grid of Ni..... 48
5.7 The plot of Total energy with degauss of Fe..... 49
5.8 The plot of Total energy with degauss of Ni..... 50
5.9 The plot of energy gap between conduction and valence band of Fe 51
5.10 The plot of energy gap between conduction and valence band of Ni 52
5.11 DOS curve of Fe with energies at DeltE=0.01..... 53
5.12 DOS curve of Ni with energies at DeltE=0.01..... 54
5.13 PDOS curve of Fe with energies at DeltE=0.01..... 55
5.14 PDOS curve of Ni with energies at DeltE=0.01..... 55

LIST OF ABBREVIATIONS

BO	:	Born Oppenheimer
CP	:	Car-Perrinello
CPMD	:	Car-Parrinello Molecular Dynamics
DFPT	:	Density Functional Perturbation Theory
DFT	:	Density Functional Theory
DOS	:	Density of State
FPMD	:	First Principle Molecular Dynamics
GGA	:	Generalized Gradient Approximation
HEG	:	Homogeneous Electron Gas
HF	:	Hartree-Fock
HK	:	Hohenberg-Kohn
KS	:	Kohn-Sham
LDA	:	Local Density Approximation
MBE	:	Molecular Beam Epitaxy
MOVPE	:	Metalorganic Vapor Phase Epitaxy
NSCF	:	Non-Self Consistent Field
PBE	:	Perdew, Burke and Ernzerhof
PDOS	:	Partial Density of State
PP	:	Pseudo Potential
PW	:	Plane Wave
QE	:	Quantum ESPRESSO
SCF	:	Self Consistent Field
XC	:	exchange Correlation

CHAPTER 1

INTRODUCTION

1.1 General Consideration

The solidification or freezing of matter may lead to formation of ordered or disordered state in which ordered state is known as crystalline state where as the disordered one is termed the amorphous state. Crystalline state refers to an infinitive array of atoms or a group of atoms. The whole volume of crystal is constructed by moving block of smallest size along its edges which block is called a unit cell. The three-dimensional structure of a crystal is built from a repetitive arrangement of the simplest structural unit, called the unit cell, just as a single tile is often a unit cell for a two-dimensional ceramic tiling pattern. It received direct experimental configuration in 1913 through the work of W. and L. Bragg, who founded the subject of X-ray crystallography and began investigation of atoms arranged in solids. Depending on the nature of the unit cell, Bragg's law is satisfied only at certain orientations of the crystal, and a beam of X-rays will then emerge from the crystal at a certain angle to the incident beam. Bragg's law requires that the diffracted radiation from different layers of unit cells be in phase [1]. Every crystal structure satisfies the requirements of a specific group of certain symmetry operation (to show visualization of motional operations performed on atoms with unit cell). Different combination of symmetry operations results in different crystal structure.

Crystal

Crystals may be classified in terms of the dominant type of chemical binding force keeping the atoms together. All these bonds involve electrostatic forces, with the chief differences among them lying in the ways in which the outer electrons of the structural elements are distributed. The distinct types of bonds that provide the cohesive forces in crystals can be classified as follows: (i) the ionic bond (ii) the covalent bond (iii) the metallic bond (iv) the van der Waals bond and (v) the hydrogen bond. We briefly discuss the different types of bonds in crystals.

The ionic bond

The electron state is little affected by the coming together of the ions to from the solid and the interaction of any two ions within the solid can be represented by the interionic potential curve of two isolated ions. At large separation the interionic potential is dominated by the long-range electrostatic interaction $\pm e^2/4\pi\varepsilon_0 r$; the +sign for two ions of same sign and -sign for ions of opposite sign [2].

The covalent bond

In the covalent bonded crystal, the binding energy is associated with the sharing of valence electrons between atoms. The states of the valence electrons are profoundly changed by the approach of the atoms to form the solid, and where an atom forms more than one bond the energy depends strongly on their relative orientation. A pair of electros is necessary feature of covalent bond, an atom cannot in general form more bonds than valence electrons. In an ideal covalent bond between two atoms the two electrons are equally shared.

The metallic bonding

Metallic bonding, which is formed when electrons are shared by all the atoms in the solid, producing a uniform "sea" of negative charge; the solids produced in this way are the usual metals.

The Vender Wall Bond

It is an additional type of bond. However, the van der Waals bond is only significant in case where other types of bonding are not possible, for example, between atoms with closed electron shell, or between saturated molecules. The physical source of this bonding is charge fluctuations in the atoms due to zero-point motion. Van der Waal forces are responsible for the bonding in molecular crystals. The bonding energy is dependent on the polarizability of the atoms involved and is mostly of order of 0.1eV. Typical atomic bonding radii for van der Waals bonding are considerably larger than for chemical bonding.

The Hydrogen Bond

In a chemical bond when a atom is bond to two other atoms. At first, it's surprising that such a bond can exist since hydrogen has just one electron. However, one can imagine the chemical bond as follows: when hydrogen takes part during a chemical bond with a strongly electronegative atom, for instance, oxygen, its single electron is nearly completely transferred to partner atom. The proton which remain can then exert a beautiful force on a second negative atom and very small size of the proton with its strongly reduced electron screening, it's impossible for a 3rd atom to be bound. Generally, speaking, the phenomena related to hydrogen bonding are quite diverse and this sort of bonding is harder to characterize than most other types. The binding energies of hydrogen bonds are of the order of 0.1eV per bond [3].

An infinite array of points in space called a lattice (space lattice) and arrangement of points defined the lattice symmetry. when an atom or a uniform group of atom s attached to each lattice point, we get a crystal structure. The attached atom or group of atoms called basis, which is identical for each lattice point in terms of composition, relative orientation, and separation. The lattice is defined by three fundamental translation vector **a**, **b** and **c** such the atomic arrangement looks an equivalent in every respect when viewing from the purpose r as when viewed from the purpose . Draw a vector **t** connecting two lattice point P1 and P2 (fig 1.1) represent vectors r_1 and r_2 respectively then, the vector t is defined as

$\vec{r}+\vec{T}=\vec{r}'$

Such that

$$\vec{t} = n_1\vec{a} + n_2\vec{b} + n_3\vec{c}$$

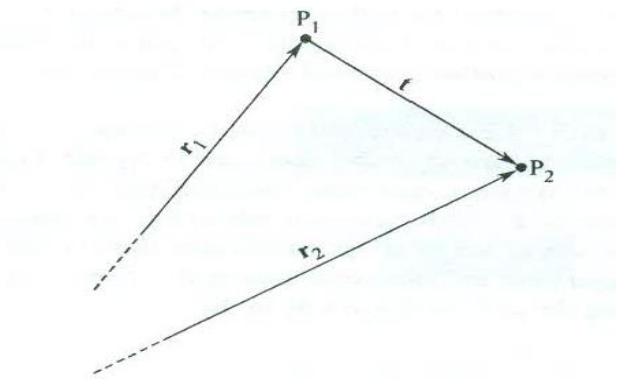

Fig. 1.1: Two lattice points P_1 and P_2 of a three-dimensional lattice connected by translation vector t [46]

When all the lattice points can be located for the arbitrary choice of only integral values of n_1, n_2 and n_3, the crystal axes **a, b** and **c** are called primitive and the resulting unit is called *primitive cell.* A lattice is a mathematical abstraction; the crystal structure is formed when a basis of atom is attached identically to every lattice point. The logical relation is

Lattice + basis = crystal structure

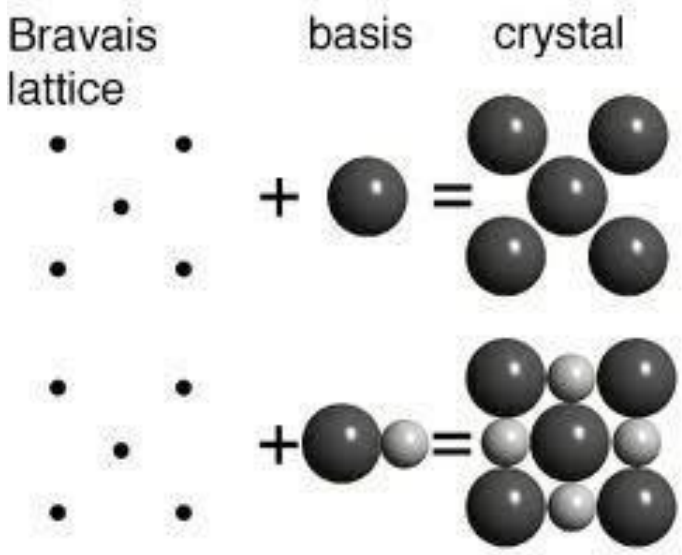

Fig 1.2: Crystal structure [47]

An alternate primitive cell is known as Wigner-Seitz cell. A lattice point is joined to all the nearby lattice point s with the help of lattice vectors. Then, a plane perpendicular to each of these vectors, connecting the central lattice point, is draw at the midpoint of the vector. The planes form a completely closed polyhedron which

contains one lattice point at the Centre which is named Wigner and Seitz [4]. Figure 1.3 shows the pictures of cell in two-dimension lattice.

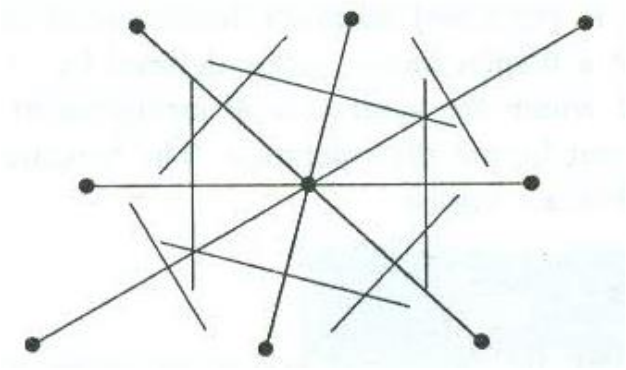

Fig.1.3: The construction of Wigner-Seitz cell for a two-dimensional space lattice[48]

Lattice planes and miller indices

A well-formed crystal or internal planes through a crystal structure are laid out in terms of Miller Indices, h, k, and l, written in round brackets, (hkl). an equivalent terminology is employed to specify planes during a lattice. Miller indices, (hkl), represent not only one plane, but the set of all identical parallel lattice planes. The values of h, k and l are the reciprocals of the fractions of a unit edge, a, b and c respectively, intersected by an appropriate plane. this suggests that a group of planes that lie parallel to a unit edge is given the index 0 (zero) no matter the lattice geometry. Thus, a group of planes that transit the ends of the unit cells, cutting the a-axis at an edge 1 a, and parallel to the b- and c-axes of the unit has Miller indices (100), (Figure 1.4a, b). an equivalent principles apply to the opposite planes shown. The set of planes that lies parallel to the a- and c-axes, and intersecting the top of every unit at an edge 1 b have Miller indices (010), (Figure 1.4c, d). The set of planes that lies parallel to the a- and b-axes, and intersecting the top of every unit at an edge 1 c have Miller indices (001), (Figure 1.4e, f). Planes cutting both the a-axis and b-axis at 1 a and 1 b are going to be (110) planes, (Figure 1.4 g, h), and planes cutting the a-, b- and c-axes at 1 a, 1 b and 1 c are going to be (111).

Remember that the Miller indices ask a family of planes, not only one . for instance , Figure 1.5 shows a part of the set of (122) planes, which cut

the unit edges at 1 a, ½ b and ½ c. The Miller indices for lattice planes are often determined employing a simple method [5].

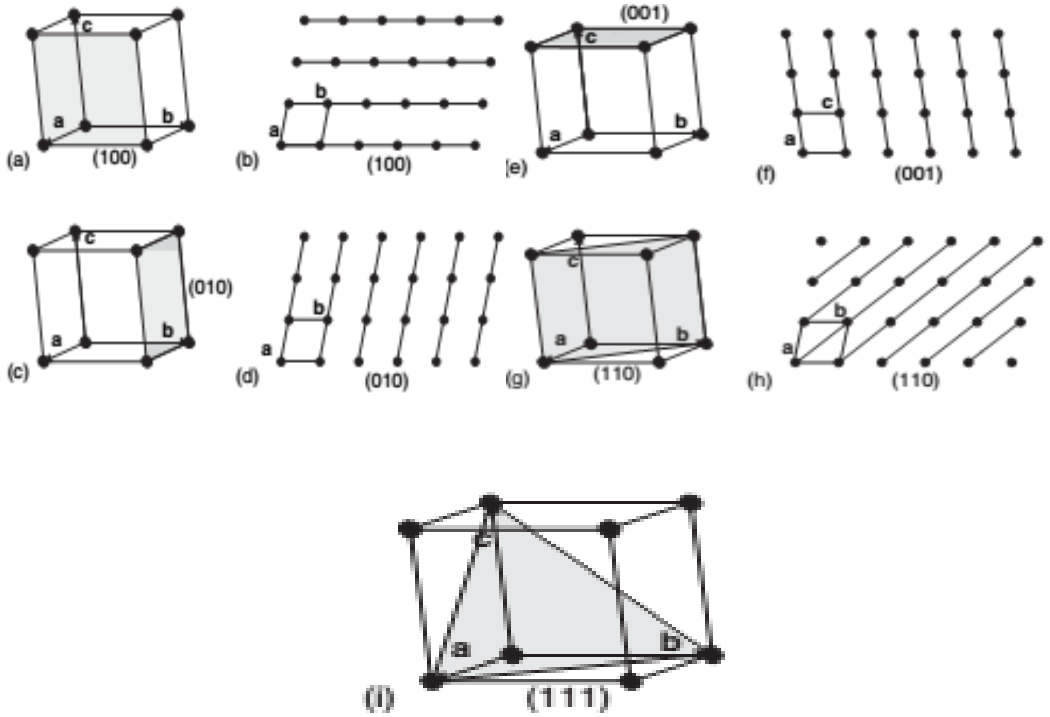

Figure 1.4 Miller indices of lattice planes: (a, b) (100); (c, d) (010); (e, f) (001), (g, h) (110); (i) (111) [49]

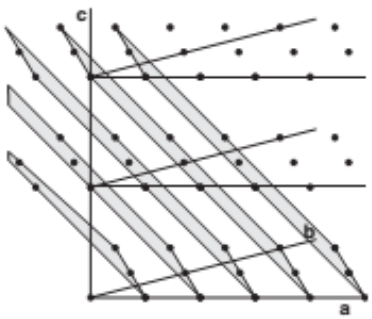

Figure 1.5: Part of the set of (122) lattice planes Bravais lattice in two dimensions [50]

The five Bravais lattice that can be received in two-dimension are depicted in fig.1.6*a* along with the primitive cell

Here they are described in terms of the elementary translation vectors $\mathbf{a}_1$ and $\mathbf{a}_2$ and of the angle ϕ that they form:

Properties

P1. Squared: $|\mathbf{a}_1| = |\mathbf{a}_2|$ and $\mathbf{a_1}$, $\mathbf{a_2}$ placed at angle $\varphi = \pi/2$

P2. Rectangular: $|\mathbf{a}_1| \neq |\mathbf{a}_2|$, and $\phi = \pi/2$

P3. Body-centered rectangular: As in the rectangular case in P2, but an extra lattice point is located at the center of each rectangle. Note that this is a cell with two lattice points, located at center and vertex positions of the rectangle. A cell including more than one lattice site and designed to have all the symmetries of the given lattice is usually named convention a cell. In particular, here the conventional cell is actually not the primitive cell. The latter can instead be represented considering the cell origin at the rectangle center and choosing a1 and a2 to be the vectors connecting the center with two vertexes of the same rectangle. In this representation, $|\mathbf{a}_1| = |\mathbf{a}_2|$ but $\phi \neq \pi/2$.

P4. Slanted or oblique: $|\mathbf{a}_1| \neq |\mathbf{a}_2|$and $\phi \neq \pi/2$.

P5. Hexagonal: $|\mathbf{a}_1| = |\mathbf{a}_2|$and $\phi = 2\pi/3$.

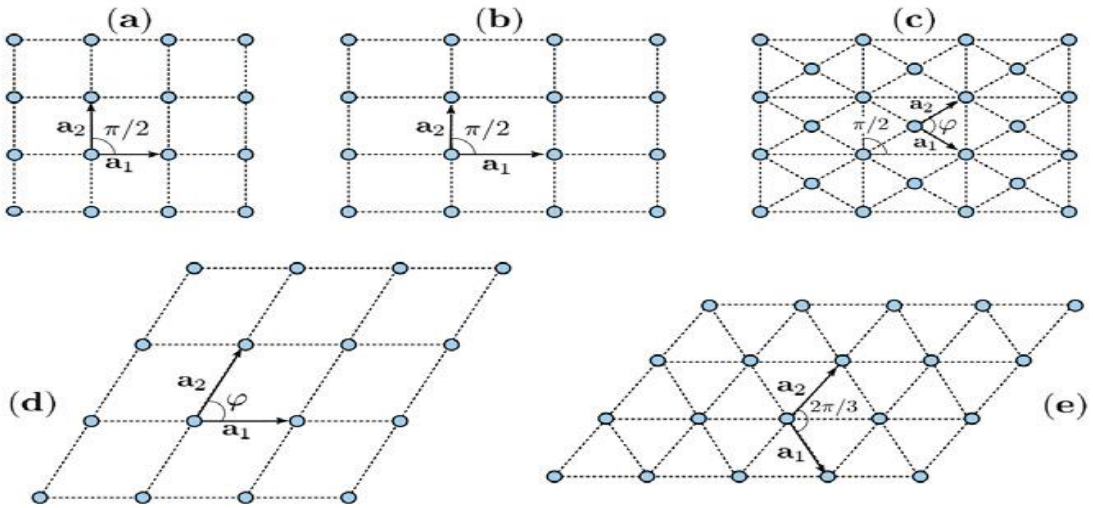

Fig. 1.6: Bravais lattice in 2D. The five conceivable Bravais lattices in 2D are depicted from (a) to (e) [51]

The point-group symmetries related to these 5 lattices are easily picked out. Starting from that with lower symmetry, the slanted lattice in P4 has binary-axes symmetries. To the above binary-axes symmetries, the rectangular P2 and the body-centered rectangular P3 add reflections with respect to the straight-dashed lines in Fig. 1.4 (b) or any other straight line parallel to the latter and crossing at the rectangles centers.

The squared lattice in P1 adds quaternary axes symmetries. Finally, the hexagonal P5 has ternary and scenery-axes symmetries, besides reflection symmetries. Note the peculiarity here that two different Bravais lattices, the rectangular and the body-centered rectangular, share the same point-group symmetry.

Three-Dimension Lattice Types

The point symmetry group in thee dimension require the 14 different lattice types listed in Table 1. The general lattice is triclinic, and there are 13 special lattices. These are grouped for convenience into systems classified according to seven types of cells, which are triclinic, monoclinic, orthorhombic, tetragonal, cubic, trigonal, and hexagonal. The division into systems is expressed in the table in terms of the axial relations that describe the cells. The cells in Fig. 6 are conventional cells: of these only the (SC) is a primitive cell. Often a non-primitive cell has a more obvious relation with the point symmetry operations than has a primitive cell. There are three lattices in the cubic system: the simple cubic (SC) lattice, the body-centered cubic (HCC) lattice, and the face-centered cubic (FCC) lattice

Cubic System

The point-group symmetries are those which leave a cube unchanged and can be counted in the number of 48. Three different Bravais lattices are classified in the cubic system: simple cubic, body-centered cubic and face-centered cubic. All of them are described below, since a great variety of materials occur in either one of these structures.

Tetragonal system

A tetragonal lattice is originated by a cube that is transformed into a parallelepiped with square base. Two different Bravais lattices are classified in the tetragonal system: simple and body-centered tetragonal lattice.

Orthorhombic system

The orthorhombic system is originated from the tetragonal one, after relaxing the requirement that the base be squared. Four different Bravais lattices are classified in the orthorhombic system: simple, base-centered, body-centered, and face-centered orthorhombic lattice.

Monoclinic system

The monoclinic system is originated from the orthorhombic ones, after making the base to be a rhomb. Two different Bravais lattices are classified in the monoclinic system, simple and face-centered.

Triclinic system

The triclinic system is originated from the monoclinic one, after slanting vector $\mathbf{a}_3$ with respect to the direction orthogonal to the plane containing $\mathbf{a}_1$ and $\mathbf{a}_2$.

Trigonal system

The trigonal system is originated from the simple cubic lattice, after deforming the cube along its diagonal: all the faces are rhombus, and each vertex is composed of three corners, each two of them forming the same angle.

Hexagonal system

The hexagonal system is obtained by layering hexagonal lattice planes one on top of the other, at distance *c*. The layering is arranged so that corresponding lattice points in adjacent planes are connected by lines perpendicular to the planes [5].

Table 1.1: Different types of lattice system [6]

System	**Bravais lattice**	**unit cell characteristics**	**Characteristics symmetry elements**
Cubic	Simple Body centered Face centered	a = b = c $\alpha = \beta = \gamma = 90°$	Four 3-fold rotation axes (along cube diagonal)
Tetragonal	Simple Body centered	a = b ≠ c $\alpha = \beta = \gamma = 90°$	One fourfold rotation axis
Orthorhombic	Simple Base centered Body centered Face centered	a≠ b ≠ c $\alpha = \beta = \gamma = 90°$	Three mutually orthogonal 2-fold rotation axes.
Monoclinic	Simple Base centered	a≠ b ≠ c $\alpha = \beta = 90° \neq \gamma$	One twofold rotation axis
Triclinic	Simple	a≠ b ≠ c $\alpha \neq \beta \neq 90° \neq \gamma$	None
Trigonal(rhombohedra)	Simple	a = b = c $\alpha = \beta = \gamma \neq 90$	One threefold rotation axis
Hexagonal	Simple	a = b = c $\alpha = \beta = 90$ $\gamma = 120$	One threefold rotation axis

The unit cell of a crystal is defined as that volume of space that its translations allow all the space without intervals and superposition to be covered. The PUC is the minimal volume V**a** = a1[a2 × a3] unit cell connected with one Bravais lattice point.

Conventional unit cells are defined by two, four and two lattice points, for the base-, face- and body-centered lattices, respectively.

Table 1.2: Characteristics of cubic lattices [7]

	Simple	body-centered	Face-centered
Volume, conventional call	a^3	a^3	a^3
Lattice Points per cell	1	2	4
Volume primitive cell	a^3	$\frac{1}{2}a^3$	$\frac{1}{4}a^3$
Lattice points per unit volume	$\frac{1}{a^3}$	$\frac{2}{a^3}$	$\frac{4}{a^3}$
Number of nearest neighbors	6	8	12
Nearest-neighbor distance	a	$3^{1/2}\,a/2 = 0.866a$	$a/2^{1/2} = 0.707a$
Number of second neighbors	12	6	6
Second neighbor distance	$2^{1/2}a$	a	a
Packing Fraction	$\frac{1}{6}\pi$=0.524	$\frac{1}{6}\pi\sqrt{3}$=0.680	$\frac{1}{6}\pi\sqrt{3}$=0.740

Miller indices

All the faces of crystal can be described and numbered in terms of their axial intercepts where, axes represent crystallographic axes which are chosen to fit the symmetry; one or more of these axes may be axes of symmetry or parallel to them, but three convenient crystal edges be used if desire. The intercept *X, Y* and *Z* of this plane on the axes *x, y* and *z* are called parameters ***a, b*** and ***c***. the ratio of parameter ***a: b*** and ***b:c*** are called the axial ratios, and by convention the values of parameters are reduced so that value of b is unity. W. H. Miller suggested in 1839, that each face of crystal could be represented by the indices *h, k* and *l,* defined by [8]

$$h = \frac{a}{X}, k = \frac{b}{Y}, l = \frac{c}{Z}$$

The Reciprocal Lattice

The set of all wave vectors K that yield plane waves with the periodicity of a given Bravais lattice is known as its reciprocal lattice. Analytically, K belongs to reciprocal lattice of Bravais lattice of point R. so we characterize the reciprocal lattice as the set of wave vectors K satisfying

$$e^{i\vec{K}.\vec{R}} = 1$$

For all R in Bravais lattice

That the reciprocal lattice is itself a Bravais lattice follow most simply from the definition of Bravais lattice. Let $\mathbf{a_1}$, $\mathbf{a_2}$, and $\mathbf{a_3}$ be a set of primitive vectors for the direct lattice. Then reciprocal lattice can be generated by three Primitive vectors

$$\overrightarrow{b_1} = 2\pi \frac{\overrightarrow{a_2} \times \overrightarrow{a_3}}{\overrightarrow{a_1}(\overrightarrow{a_2} \times \overrightarrow{a_3})}$$

$$\overrightarrow{b_2} = 2\pi \frac{\overrightarrow{a_3} \times \overrightarrow{a_1}}{\overrightarrow{a_1}(\overrightarrow{a_2} \times \overrightarrow{a_3})}$$

$$\overrightarrow{b_3} = 2\pi \frac{\overrightarrow{a_1} \times \overrightarrow{a_2}}{\overrightarrow{a_1}(\overrightarrow{a_2} \times \overrightarrow{a_3})}$$

To verify above equation gives a set of primitive vectors for the reciprocal lattice, one first note that the $\mathbf{b_i}$ satisfy

$$b_i . a_j = 2\pi\delta_{ij},$$

Where δ_{ij} is the Kronecker delta symbol

$$\delta_{ij} = 0, i \neq j,$$

$$\delta_{ij} = 1, i = j,$$

Since the reciprocal lattice is itself a Bravais lattice.

The reciprocal of reciprocal lattice is the set of all vectors **G** satisfying

$$e^{i\vec{G}.\vec{K}} = 1$$

For all K in reciprocal lattice, where $K = k_1 b_1 + k_2 b_2 + k_3 b_3$ [9]

The Brillouin zone construction gives the all wave vectors which suffer diffraction from the crystal [10]. The first Brillouin zone has the shape of the truncated octahedron.

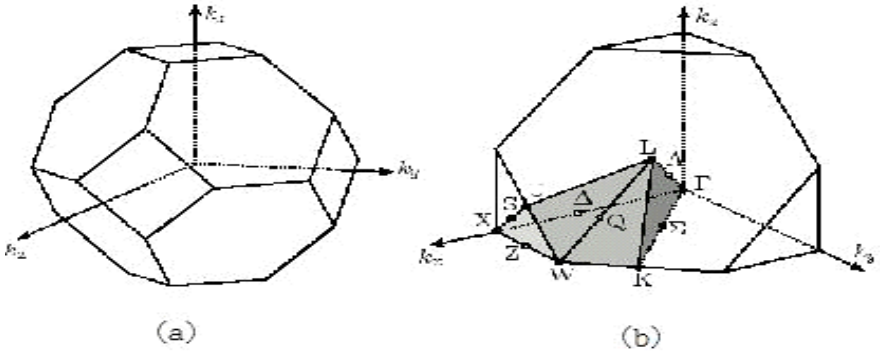

Figure 1.7: Brillouin zone [52]

Density of states

We may find the number of energy levels $dN(E)$ within energy interval E and $E + dE$ (or with n between n and $n + dn$) by counting the number of points that lie in a spherical shell or radius E and thickness dE. It may be noted here that although the energy E (and therefore n) is quantized, the spacing between the successive energy levels becomes infinitesimally small as L becomes large. We can then treat E and therefore n as continuous variables. Then energy interval dE corresponds to an interval dn given by

$$dE = \frac{\hbar^2\pi^2}{2mL^2} \times 2ndn,$$

Now the number of points in the positive octant of a spherical shell of radius n and thickness dn is $dN = \frac{1}{8} \times 4\pi n^2 dn$. we find

$$dN(E) = \frac{1}{4\pi^2}\left[\frac{2m}{\hbar^2}\right]^{\frac{3}{2}} L^3\sqrt{E}dE = \frac{1}{4\pi^2}\left[\frac{2m}{\hbar^2}\right]^{\frac{3}{2}} V\sqrt{E}dE$$

Where, V is the volume of the box (occupied by the system).

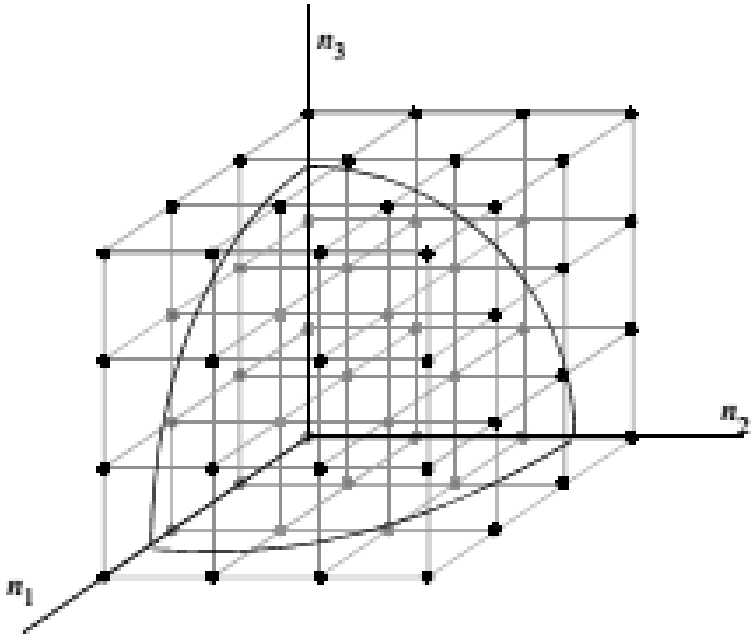

Fig 1.8: When a particle is enclosed in cubical box of dimension L the energy levels are discrete [53]

Each energy state corresponds to a point in three-dimensional (n_1, n_2, n_3)space in the positive octant. The spacing between the successive energy levels can be made as small as desired by choosing *L* sufficiently large [11].

1.2 Study Material: Iron and Nickel

Iron is a transition element with symbol Fe and atomic number 26. It lies in group 8 and period 4 in the periodic table. Humans started to extracted in Eurasia only about 2000BCE and use of iron tools and weapons began to displace copper alloys only around 1200BC [10]. The body of an adult human contains about 4 grams(0.005% body weight) of iron, mostly in hemoglobin and myoglobin. At least four allotropes of iron (differing atom arrangements in the solid) are known, conventionally denoted α, γ, δ and ε. The melting point of iron is experimentally well defined for pressures less than 50 Gpa which is along with enthalpy of atomization [32]. Below its Curie point of 770°C, α-iron changes from paramagnetic to ferromagnetic: the spin of two unpaired electrons in each atom generally align with the spin of its neighbors, creating an overall magnetic field .It has four stable isotopes: ^{54}Fe,^{56}Fe,^{57}Fe and ^{58}Fe.Iron found in rocky planets like Earth is due to its abundant production by fusion in high-mass stars, where it is the last element to be produced with release of energy before the violent collapse of a supernova, which scatters the iron into space. Most of the iron

in the crust is combined with various other elements to form many iron minerals. An important class is the iron oxide minerals such as hematite(Fe_2O_3), magnetite(Fe_3O_4) and siderite($FeCO_3$) . Iron and its compound is used in various sector like food diet, steel making, structural material etc. [32]

Because the ores of nickel are easily mistaken for ores of silver, understanding of this metal and its use dates to relatively recent times. However, the unintentional use of nickel is ancient, and can be traced back as far as 3500 BCE[10]. Bronzes from what is now Syria have been found to contain as much as 2% nickel. Some ancient Chinese manuscripts suggest that "white copper" (cupronickel, known as baitong) was used there between 1700 and 1400 BCE. This Paktong white copper was exported to Britain as early as the 17th century, but the nickel content of this alloy was not discovered until 1822 [39]

It was discover by Baron Axel Frederik Cronstedt in 1751. Nickel is a chemical element with the symbol Ni and atomic number 28 with highly reactive but larger pieces are slow to react with air under standard conditions because an oxide layer forms on the surface and prevents further corrosion (passivation). Even so, pure native nickel is found in Earth's crust only in tiny amounts, usually in ultramafic rocks and in the interiors of larger nickel–iron meteorites that were not exposed to oxygen when outside Earth's atmosphere[45]. Nickel is a silvery-white metal with a slight golden tinge that takes a high polish. It is one of only four elements that are magnetic at or near room temperature. Its Curie temperature is 355°C (671°F), meaning that bulk nickel is non-magnetic above this temperature. The unit cell of nickel is a face-centered cube with the lattice parameter of 0.352nm, giving an atomic radius of 0.124nm .It have five stable isotopes ^{58}Ni,^{60}Ni,^{61}Ni,^{62}Ni and ^{64}Ni . On Earth, nickel occurs most often in combination with sulfur and iron in pentlandite, with sulfur in millerite, with arsenic in the mineral nickeline, and with arsenic [34]

1.2.1 Crystal Structure

Iron and Nickel can take shape in different gem structures. In any case, every change is just steady inside specific temperature ranges. The total change from one into another precious stone structure is called allotropic change; the particular change temperature is known as the transus temperature. Iron has two different crystal structure at atmospheric pressure: the body centered cubic (bcc) and the face centered

cubic (fcc).In ground state the bcc α-phase is stable and at the temperature T=1184K (A_3 point), α-Fe transforms into fcc α-Fe, which is stable up to 1665K (A_4 point). Above this temperature, iron transforms back into the bcc phase (σ-Fe), which remains stable up to the melting point T_m=1809K. Since α and σ Fe are isomorphic, the two are usually not distinguished when referred to bcc Fe. Steels with bcc and fcc structures are usually referred to as "ferrite" and "austenite" respectively. The boiling point of iron is about 3300K and third form of iron which has the hexagonal close packed (hcp) structure, can be stabilized under high pressures. The melting and boiling point of Fe is 1538 °C and 2861 °C with specific gravity 7.874 and atomic radius 156pm[32]

Nickel is a silvery-white metal with a slight golden tinge that takes a high polish. It is one of only four elements that are magnetic at or near room temperature, the others being iron, cobalt and gadolinium. Its Curie temperature is 355°C (671°F), meaning that bulk nickel is non-magnetic above this temperature.[39] The unit cell of nickel is a face-centered cube with the lattice parameter of 0.352nm, giving an atomic radius of 0.124nm. This crystal structure is stable to pressures of at least 70GPa. Nickel belongs to the transition metals. It is hard, malleable and ductile, and has a relatively high electrical and thermal conductivity for transition metals [34]

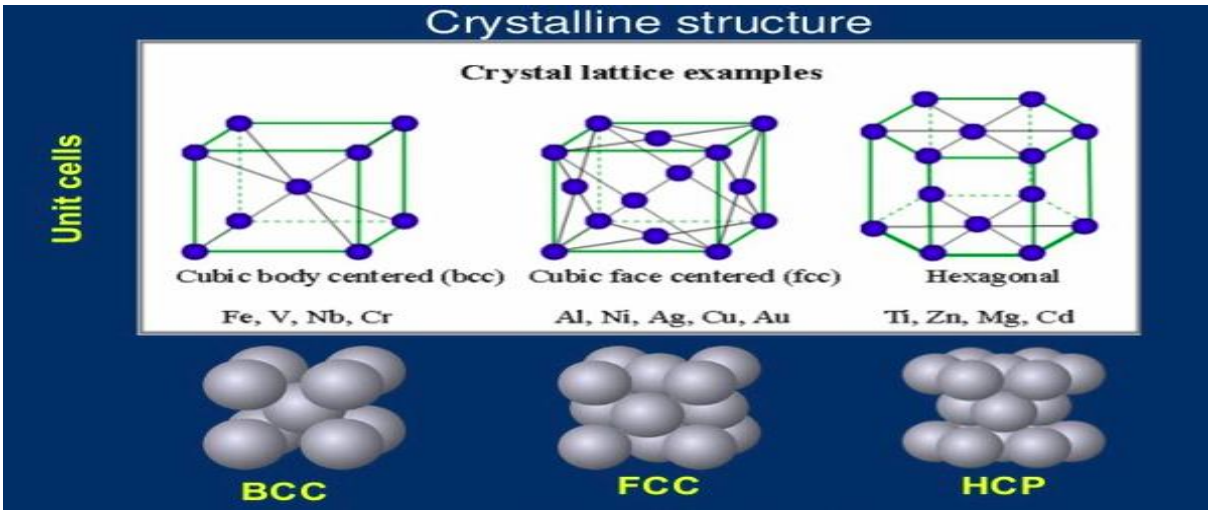

Fig. 1.9: Crystal structure of bcc, fcc and hcp phase [54]

Iron and Nickel introduction in short

Table 1.3: Introduction of Fe and Ni

Titles	**Concerned(values ,formulas and others)**	
1. symbol	Fe	Ni
2. Group	8	10
3 .Block	d	d
4.Atomic number	26	28
5.density	7.874 gcm^{-3}	8.908gcm^{-3}
6.melting point	1811 k	1728k
7.Boiling point	3134 k	3186k
8. Relative atomic mass	55.845	58.6934
9.Specific heat capacity	449J/(kg K)	445J/(kg K)
10.Stable Isotopes	^{56}Fe	^{58}Ni
11. Electron Configuration	[Ar] $4s^2$ $3d^6$	[Ar] $4s^2$ $3d^8$
12. Curie point	1043 K	631 K

1.2.2 Scope of the Present Work

The study of properties of solid is one of the most interesting and fruitful branches of physics. By knowing the lattice dynamics, we can predict different physical properties of solid and help to uses these solid in daily life application, which we can easily observed in this time period.

In this present work, we have studies the density of state (DOS) of transition metal Iron and Nickel. From the study of DOS, we can get idea about nature of the solid and magnetic properties.

The main objectives of our study are:

1. To study about the crystal structure done by previous worker.

2. To estimate the lattice parameter of Fe and Ni.

3. To study and plot the density of state of Fe and Ni.

1.3 How we Approach?

Mainly this research work is done is computational by using Quantum ESPRESSO (QE) package. First, we optimized structure of Transition metal by optimizing lattice parameters, then we study the band structure, DOS and PDOS of Iron And Nickel. In this study, we choose bcc structure for iron and fcc structure for nickel because of its computational cost and simplicity of structure.

The outline of the present work is summarized follows:

In this work, Chapter 1 includes general introduction about crystal structure and lattice dynamics with attachment of objective and scope of work. In chapter 2, we discuss the literature review of the elements Iron and Nickel. In chapter 3, we discuss the theoretical models of the method employed in calculations such as Born-Oppenheimer, Hartree-Fock method, Density functional theory with local density approximation (LDA), General gradient approximation (GGA) and Pseudo potential. In chapter 4 we described some detail about Quantum ESPRESSO and its execution. Then in chapter 5 we discuss and present about main finding of this research. Finally, in chapter 6 we summarize our results and mention about further advantage of same field research. References are listed at end of chapter 6.

CHAPTER 2

LITERATURE REVIEW OF IRON AND NICKEL

In 1986 **Tashi Nautiyal and Sushil Auluck** study about Electronic structure of ferromagnetic iron: Band structure and optical properties and in which a theoretical study of the band structure, density of states, and the optical properties of ferromagnetic iron is presented by using first principle[35]

In 1989 **L.M Sandratskii, P.G. Gulestskii** study about Energy band structure of BBC iron at finite temperatures by Using the KKR method generalized for the case of non-collinear spin structures, and calculated the electron spectrum, the density of states, and the total energy of a number of helical magnetic configurations for bcc iron.[36]

In 2018 **Vivek Kumr Jain, N.Lakshmi, Rakesh Jin and Aarti Rani Chandra** published an article Electronic Structure, Elastic, Magnetic, and Optical Properties ofFe_2MnZ (*Z*= Si, Ge, and Sn) Full Heusler Alloys: First-Principle Calculations where Investigations of the electronic structure, elastic, magnetic, and optical properties of Fe_2MnZ full Heusler alloys show mechanical stability with cubic symmetry in all three alloys.[37]

In 1997 **Carme Rovira, Karel Kunc, Jürg Hutter, Pietro Ballone, and Michele Parrinello** published an article of Equilibrium Geometries and Electronic Structure of Iron−Porphyrin Complexes: A Density Functional Study in which performed density functional theory (DFT) calculations of iron−porphyrin (FeP) and its complexes with O2, CO, NO, and imidazole (Im).[38]

The energy band structure of nickel was first investigate by **Slater (1936)** is an attempt to explain the occurrence of ferromagnetism in this material. He obtained a density of states for nickel by an extrapolation from the energy bands of copper, which had been calculated by **Krutter(1935)** using the cellular method of **Wigner and Seitz(1933)** by the modified tight-binding approximation and the Green's function method.[39]

In 1974 C. S. **Wang and J. Callaway** published an article Band structure of nickel: Spin-orbit coupling, the Fermi surface, and the optical conductivity in which previous self-consistent calculation of energy bands in ferromagnetic nickel using the tight-binding method has been extended to include spin-orbit coupling.[40]

In 1978 N.I .**Kulikov, V.N. Borzunov, and A.D. Zvonkov** published a paper The electronic band structure and interatomic bond in nickel and titanium hydrides in which Using an approximation for solving the Korringa-Kohn-Rostoker equation the band structure of titanium and nickel di-hydrides and nickel hydride are calculated. The results are compared with experimental data [41]

CHAPTER 3

THEORY

3.1 General consideration

Determination of the electronic structure of solids is a many-body problem that requires the Schrödinger equation to be solved for an enormous number of nuclei and electrons. Even if we managed to solve the equation and find the complete wave function of a crystal, we face the not less complicated problem of determining how this function should be applied to the calculation of physically observable values. While the exact solution of the many-body problem is impossible, it is also quite unnecessary.

3.2 Born-Oppenheimer approximation

To describe the various motions of the molecule we begin with the Schrodinger equation. The Hamiltonian is given by

$$\hat{H} = \hat{T}_e + \hat{T}_N + V_{ee} + V_{eN} + V_{NN}, \tag{2.1.1}$$

Where

$$\hat{T}_e = \sum_{i=1}^{N} \frac{\hat{p}_i^2}{2m} \tag{2.1.2}$$

Represents the kinetic energy of the electrons and

$$\hat{T}_N = \sum_{v=1}^{2} \frac{\hat{p}_v^2}{2M_v} \tag{2.1.3}$$

is the kinetic energy of the nuclei. V_{eN} Represents the attractive electron-nuclei potential. V_{ee} Describes the repelling electron-electron interaction. V_{NN} indicates the repelling Coulomb interaction between the nuclei. Since the masses of the nuclei are very large, $\hat{T}_N$ can be neglected. This step is called the Born-Oppenheimer approximation. In the following, we will explain the ap- proximation in more detail.

If we neglect the kinetic energy $\hat{T}_N$ of the nuclei (static approximation: fixed distance R of the nuclei), the relative distance R between the nuclei only occurs as a parameter. The Schrodinger equation becomes

$$\left[\hat{T}\middle|e + V_{ee}(r) + V_{eN}(r,R)\right]\varphi_n(r,R) = [\varepsilon_n(R) - V_{NN}(R)]\varphi_m(r,R). \qquad (2.1.4)$$

Here r indicates the position of the electron. The solutions $\varphi_n(r,R)$ depend parametrically on the distance between the nuclei. The energy of this state is given by the electronic energy $\varepsilon_n(R)$ lowered by $V_{NN}(R)$. The solutions $\varphi_n(r,R)$ represent a complete set of functions. The true wavefunction $\psi(r,R)$ can be expanded within this set:

$$\psi(r,R) = \sum_m \phi_m(R)\,\varphi_n(r,R). \qquad (2.1.5)$$

The coefficients $\phi_m(R)$ are to be found and, in general, depend on R. $\varphi_n(r,R)$ is the solution of the full Schrodinger equation, which takes into consideration the kinetic energy $\hat{T}_N$ of the atomic nuclei, i.e.

$$\left(\hat{T}\middle|e + \hat{T}_N + V_{ee} + V_{eN} + V_{NN}\right)\psi(r,R) = E\psi(r,R) \qquad (2.1.6)$$

Inserting (2.1.5) into (2.1.6) and using (2.1.4), we obtain

$$\sum_m\left(\varepsilon_m(R) + \hat{T}_N\right)\phi_m(R)\,\varphi_n(r,R) = E\sum_m \phi_m(R)\varphi_m(r,R) \qquad (2.1.7)$$

Now we multiply from the left-hand side with ${\varphi^\dagger}_n(r,R)$, integrate over the full space, and get

$$\sum_m \int\int d^3r\,{\varphi^\dagger}_n(r,R)\hat{T}_N\,\phi_m(R)\varphi_m(r,R) + \varepsilon_m(R)\phi_n(R) = E\phi_n(R). \qquad (2.1.8)$$

Here we have used the orthogonally of the functions$\varphi_m(r,R)$. $\hat{T}_N$ is proportional to the Laplace operator Δ_R, which acts on $\varphi_m\varphi_m$. It holds that

$$\Delta_R(\phi\varphi) = (\Delta_R\phi)\varphi + 2\Delta_R\Phi.\,\Delta_R\varphi + \phi\Delta_R\varphi. \qquad (2.1.9)$$

The index R indicates the action of the operators in R space. The first term in (2.1.9) is proportional to $\hat{T}_N\phi_n$. The rest is brought to the right-hand side of (2.1.8). The result reads

$$\left[\hat{T}_N + \varepsilon_n(R)\right]\phi_n(R) = E\phi_n(R) - \sum_m C_{nm}\phi_m(R) \qquad (2.1.10a)$$

With

$$C_{nm}\phi_m(R) = -\hbar^2 \sum_{\alpha} \frac{1}{2M_\alpha} \int \; d^3r \, \varphi^{\dagger}{}_n(r,R) \times$$

$$\left[2\nabla_{R_\alpha}\phi_m(R).\nabla_{R_\alpha}\varphi_m(r,R) + \phi_m(R)\nabla_{R_\alpha}\varphi_m(r,R)\right]. \qquad (2.1.10b)$$

The sum over a comes from $\hat{T}_N$ and ∇_{R_α} acts only on the co-ordinate R_α of the nucleusα, which appears in $R = \sqrt{(R_2 - R_1)^2}$. Now, the order of magnitude of C_{nm} is $(m/M)^{1/2}$ times smaller than the electronic kinetic energy. This can be seen as follows. The order of magnitude of the term ~ $\hbar^2\nabla_{R_\alpha}\varphi_m/2M_\alpha$ (the kinetic energy of the nucleus) is proportional to $-(m/M_\alpha)\hbar^2(\nabla_r \varphi_m/2\,m)$; we have simply replaced ∇_{R_α} by ∇_r and introduced the electronic kinetic energy $\hbar^2\nabla_{R_\alpha}\varphi_m/2M_\alpha$. The factor m/Ma indicates that the contribution of ∇_{R_α} to C_{nm} is smaller by this factor than the kinetic energy of the electron.

The first term in (2.1.10b) remains to be estimated. For this we approximate ϕ_m by a harmonic oscillator wavefunction: $\phi_m \approx exp$,R_0 being the equilibrium position of nucleus α. We have

$$\nabla_{R_\sigma}\phi_m \approx |R - R_0|\frac{M\omega}{\hbar}\phi_m \approx \frac{(\delta R)M\omega}{\hbar}\phi_m \qquad (2.1.11)$$

δRindicates the shift from the equilibrium position. The factor *M* is cancelled by *1/M* in (2.1.10b) and the contribution is proportional to the vibrational energy$\hbar\omega$. As noted earlier, this goes like ~ $(m/M)^{1/2}$. As a summary, the C_{nm} term can be neglected or treated with the help of perturbation theory. Without the C_{nm} term, (2.1.10a) reduces to

$$\left[\hat{T}_N + \varepsilon_n(R)\right]\phi_n(R) = E\phi_n(R) \qquad (2.1.12)$$

This equation has an interesting interpretation: the energy of the electron states $\varepsilon_n(R)$ acts like an effective potential in *R*. We imagine that the electrons build a "medium" in which the atomic nuclei move. This medium acts as an elastic band. If the nuclei try to leave the equilibrium position, they will be drawn back. There is an equilibrium position where $\varepsilon(R)$ has a minimum deep enough to generate binding. The elastic band behaviour is then nothing other than the expansion up to the order $(R - R_0)^2$.

The C_{nm} produce a mixing between different statesφ_n and φ_m. This mixing between the $\varphi_n(R)$ stages can be neglected in lowest order, because the C_{nm} are small [of order $(m/M)^{1/2}$, as explained previously]. Accordingly, the wave function is approximately given by

$$\psi_{nv}(r,R) = \phi_{nv}(R)\varphi_n(r,R) \qquad (2.1.13)$$

Here *v* stands for all quantum numbers of level *n*. E_{nv} indicates the energy of the molecule, which is calculated from (2.1.12).

In order to describe vibrations and rotations of the molecule $\varepsilon_n(R)$ is expanded in coordinates describing vibration and rotation, respectively. The expansion in $\delta R = |R - R_0|$ up to the squared order leads to a harmonic vibrational potential (see Fig. 12.1). $\varepsilon_N(R)$does not depend on the angles (Euler angles). Hence the rotations of the molecule are free. An excitation of the molecule is a combination of excitations of the harmonic vibrational oscillator and of the rotations.

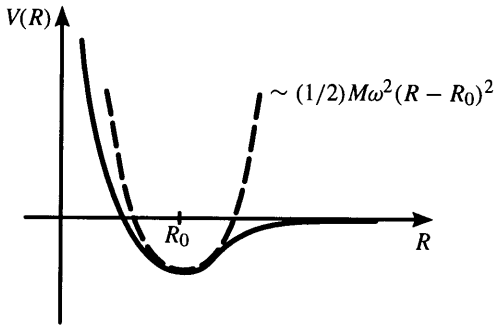

Fig. 3.1: Typical molecular potential for the nuclei in the molecule. Ro characterizes the relative equilibrium position of the two nuclei. R represents the relative nuclear distance [55]

We summarize: in the Born-Oppenheimer approximation, first the energy levels of the electrons are determined for fixed distances *R* of the nuclear centers. The electron energy $\varepsilon_n(R)$plays the role of a potential, in which the nuclei are moving. If this potential has one or several deep enough minima, one or several bound states of the molecule can exist. If the minima are only weak or do not exist at all, then the molecule is not bound.

3.3 Hartree-Fock Approximation

The simplest approach is to assume a specific form for the many-body wave function which would be appropriate if the electrons were non-interacting particles, namely

$$\psi^H(\{r_i\}) = \phi_1(r_1)\phi_2(r_2) \ldots \ldots \phi_N(r|N) \tag{2.1.14}$$

with the index *r*unning over all electrons. The wave functions $\phi_i(r_i)$ are states in which the individual electrons would be if this were a realistic approximation. These are single-particle states, normalized to unity. This is known as the Hartree-approximation (hence the superscript H). With this approximation, the total energy of the system becomes

$$E^H = \langle \Psi^H | H | \Psi^H \rangle$$

$$\sum_i \left\langle \phi_i \left| \frac{-\hbar^2 \nabla_r^2}{2m_e} + V_{ion}(r) \right| \phi_i \right\rangle + \frac{e^2}{2} \sum_{ij(j\neq i)} \tag{2.1.15}$$

Using a vibrational argument, we obtain from this the single-particle Hartree equations:

$$\left[\frac{-\hbar^2 \nabla_r^2}{2m_e} + V_{ion}(r) + e^2 \sum_{j\neq i} \left\langle \phi_j \vee \frac{1}{|r-r'|} \phi_j \right\rangle \right] \phi_i(r) + \epsilon_i \phi_i(r) \tag{2.1.16}$$

where the constants $\epsilon_i$are Lagrange multipliers introduced to take into account the normalization of the single-particle states ϕ_i(the bra $\phi_i \vee$ and ket $|\phi_i >$notation for single-particle states). Each orbital $\phi_i(r)$ can then be determined by solving the corresponding single-particle Schrödinger equation, if all the other orbitals $\phi_j(r_j), j \neq i$were known. In principle, this problem of self-consistency, i.e. the fact that the equation for one $\phi_i$depends on all the other ϕ_j's, can be solved iteratively. We assume a set of ϕ_i's, use these to construct the single-particle hamiltonian, which allows us to solve the equations for each new ϕ_i we then compare the resulting ϕ_i's with the original ones, and modify the original ϕ_i's so that they resemble more the new ϕ_i's. This cycle is continued until input and output ϕ_i's are the same up to a toleranceδ_{tol}, as illustrated in Fig. 2.2 (in this example, the comparison of input and output wavefunctions is made through the densities, as would be natural in Density Functional Theory, discussed below). The more important problem is to determine how realistic the solution is. We can make the original trial ϕ's orthogonal, and

maintain the orthogonality at each cycle of the self-consistency iteration to make sure the final ϕ's are also orthogonal. Then we would have a set of orbitals that would look like single particles, each $\phi_i(r)$ experiencing the ionic potential $V_{ion}(r)$ as well as a potential due to the presence of all other electrons, $V_i^H(r)$given by

$$V_i^H(r) = +e^2 \sum_{j \neq i} \left\langle \phi_j \vee \frac{1}{|r-r'|} \phi_j \right\rangle \tag{2.1.17}$$

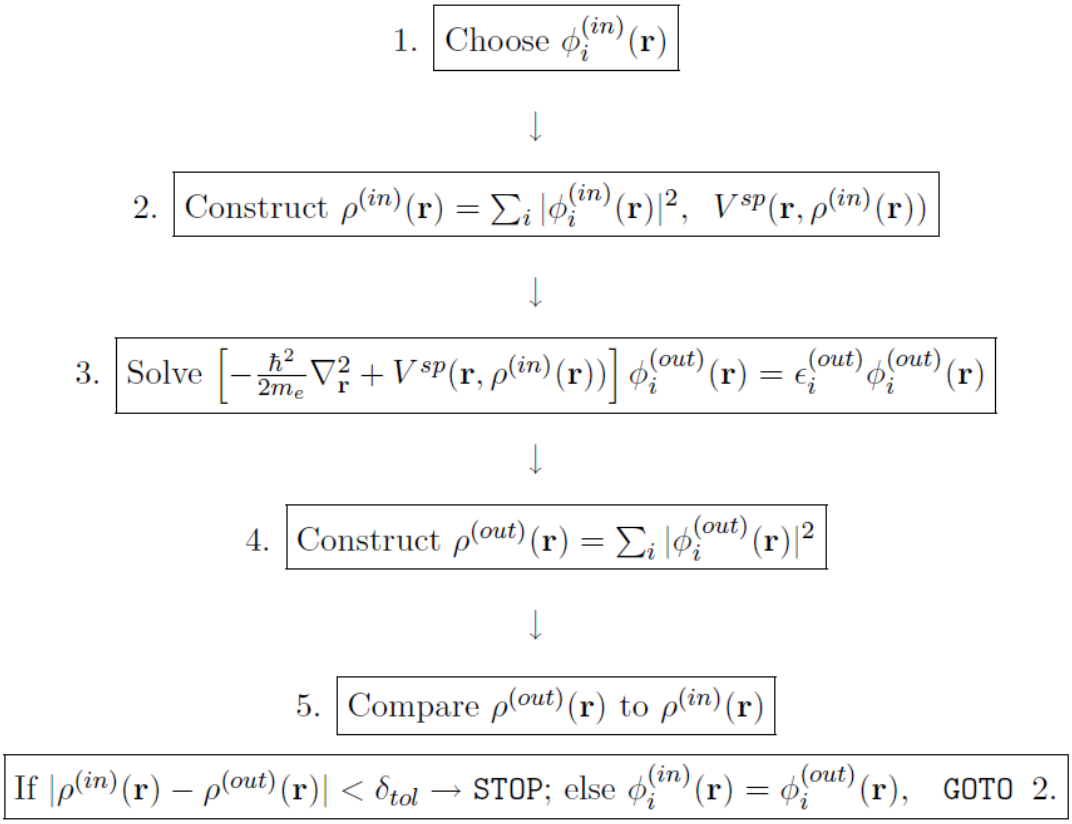

Figure 3.2: Schematic representation of iterative solution of coupled single-particle equations. This kind of operation is easily implemented on the computer [56]

This is known as the Hartree potential and includes only the Coulomb repulsion between electrons. The potential is different for each particle. It is a mean-field approximation to the electron–electron interaction, taking into account the electronic charge only, which is a severe simplification [16].

3.4 Density functional theory

There are numerous fields inside the physical sciences and building where the way to scientific and mechanical advancement is understanding and controlling the properties of *issue at the degree of individual iotas and particles. Thickness utilitarian hypothesis is an incredibly fruitful way to deal with finding answers for the essential condition that depicts the quantum conduct of ion as and atoms, the Schrödinger condition, in settings of down to earth esteem. This methodology has quickly developed from being a specific workmanship rehearsed by few physicists and scientific experts at the front line of quantum mechanical hypothesis to a device that is utilized normally by huge quantities of analysts in science, material science, materials science, substance building, topography, and different controls. A hunt of the Science Citation Index for articles distributed in 1986 with the words "thickness useful hypothesis" in the title or dynamic yields under 50 passages. Rehashing this quest for 1996 and 2006 gives more than 1100 and 5600 passages, separately [17]. Right now, start an audit of some key thoughts from quantum mechanics that underlie DFT (and different types of computational science).

The whole field of thickness useful hypothesis lays on two basic numerical hypotheses demonstrated by Kohn and Hohenberg and the inference of a lot of conditions by Kohn and Sham in the mid-1960s [17].The first theorem, proved by Hohenberg and Kohn, is: The ground-state vitality from Schrödinger's condition is a one of a kind utilitarian of the electron thickness.

Tragically, in spite of the fact that the first Hohenberg–Kohn hypothesis thoroughly demonstrates that a practical of the electron thickness exists that can be utilized to tackle the Schrödinger condition, the hypothesis says nothing regarding what the utilitarian really is. The second Hohenberg–Kohn hypothesis defines a significant property of the practical: The electron thickness that limits the vitality of the general utilitarian is the genuine electron thickness comparing to the full arrangement of the Schrödinger condition. In the event that the "genuine" utilitarian structure were known, at that point we could fluctuate the electron thickness until the vitality from the practical is limited, giving us a solution for finding the significant electron thickness. This vibrational guideline is utilized by and by with surmised types of the useful.

3.5 The Kohn-Sham approach

While the Hohenberg–Kohn theorem rigorously establishes that we may use the density and therefore the density alone, as a variable to find the ground-state energy of an N-electron problem, it does not provide us with any useful computational scheme. This is provided by the Kohn–Sham formalism. Let us then start by considering a non-interacting *N*-electron system in an external potential V_s. The Hamiltonian H_s of this system is given by:

$$H_s = T + V_s \tag{2.1.18}$$

We then apply the Hohenberg–Kohn theorem to the present system. Accordingly, there exists a unique energy functional

$$\mathcal{E}_s[n] = T[n] + \int V_s(r)n(r)\,dr \tag{2.1.19}$$

We note here that $T_s[n]$ is the kinetic energy functional of a system of N noninteracting electrons. The ground-state density of this system is easily obtained. It is simply

$$n_s(r) = \sum_{i=1}^{N}|\phi_i(r)|^2 \tag{2.1.20}$$

where we have occupied the N single-particle states, or orbitals, that satisfy the Schrödinger-like equation

$$\left[\frac{-\hbar^2}{2m}\nabla^2 + V_s\right]\phi_i(r) = \mathcal{E}_i\phi_i(r), \mathcal{E}_1 \leq \mathcal{E}_2 \leq \mathcal{E}_3 \ldots, \tag{2.1.21}$$

and have the *N* lowest eigenvalues $\mathcal{E}_i$. But we are really interested in a system of *N* interacting electrons in an external potential V_{ext}, so the question we would like to answer is the following: can we determine the form that V_s (the external potential of the non-interacting system) must take in order for the non-interacting system to have the same ground-state density as the interacting system in the external potential V_{ext}? The strategy we use is to solve for the density using the auxiliary noninteracting system, and then insert this density (which by construction is the same as that for the interacting system) in an approximate expression for the total energy of the interacting system. The first step in this process is to rewrite the energy functional $\mathcal{E}[n]$ of the interacting system, which was given in Eq. (2.1.21), as

$$\mathcal{E}[n] = T_s[n] + \left\{T[n] - T_s[n] + V[n] - \frac{e^2}{2}\iint \frac{n(r)n(r')}{|r-r'|}drdr'\right\}$$
$$+\frac{e^2}{2}\iint \frac{n(r)n(r')}{|r-r'|}drdr' + \int n(r)\,V_{ext}(r)dr$$

$$\equiv T_s + \frac{e^2}{2}\iint \frac{n(r)n(r')}{|r-r'|}drdr' + \iint n(r)\,V_{ext}(r)dr + \mathcal{E}_{XC}[n], \quad (2.1.22)$$

Here we have added and subtracted both the kinetic energy functional $T_s[n]$ of a noninteracting system and the direct, or Hartree, term in the electrostatic energy. We have then defined the sum of the terms in braces to be the exchange-correlation energy functional $\mathcal{E}_{XC}[n]$ is

$$\mathcal{E}_{XC}[n] \equiv F_{HK}[n] - \frac{e^2}{2}\iint \frac{n(r)n(r')}{|r-r'|}drdr' - T_s[n], \qquad (2..1.23)$$

We have thus swept all our ignorance about electron interactions beyond the Hartree term under the rug that we call $\mathcal{E}_{XC}[n]$. What we gain in writing $\mathcal{E}_{XC}[n]$ this way is that we can eventually focus on developing reasonable approximations for $\mathcal{E}_{XC}[n]$. According to the Hohenberg–Kohn theorem, the density n that minimizes the functional $\mathcal{E}[n]$ is the ground-state density. Thus, by taking the variation of Eq. (2.1.22) with respect to the particle density we obtain

$$\frac{\delta\mathcal{E}[n]}{\delta n(r)} = \frac{\delta T_s[n]}{\delta n(r)} = e^2\int \frac{n(r')}{|r-r'|}dr' + V_{ext}(r) + v_{xc}[n(r)] = 0, \qquad (2.1.24)$$

where we have formally defined the exchange-correlation potential as

$$v_{xc}[n(r)] \equiv \frac{\delta\mathcal{E}_{xc}[n]}{\delta n(r)}.$$

We now use the auxiliary non-interacting system and its Schrödinger equation, from which we are able to similarly show that

$$\frac{\delta T_s[n]}{\delta n(r)} + V_s(r) = 0.$$

By comparing this result with Eq. (2.5.6) we see that this ejective potential V_s (r) must satisfy

$$V_s(r) = V_{ext}(r) + e^2\int \frac{n(r')}{|r-r'|}dr' + v_{xc}(r), \qquad (2.1.25)$$

We are now doing a position to implement the self-consistent Kohn–Sham scheme. We first choose an initial trial form of the function $n(\mathbf{r})$ and substitute into Eq. (2.1.25) to find a trial form of V_s. We then solve Eq. (2.1.19) for the single-particle wave functions$\phi_i(r)$, and use Eq. (2.1.18) to find the next iteration for $n(\mathbf{r})$. When this procedure has been repeated a sufficient number of times that no further changes occur, then a solution for $n(\mathbf{r})$ has been found that not only satisfies the Schrödinger equation for the reference non-interacting electrons, but also is the correct density for the interacting system. We close this section by highlighting a few points about the Kohn–Sham formalism. First of all, it is formally exact, supposing that we can find the exact exchange-correlation potential $v_{xc}(r)$. Second, we have cast the solution of the interacting *N*-electron problem in terms of non-interacting electrons in an external potential $V_s(r)$. This is of great practical importance. The ground state wavefunction of the noninteracting system is just a Slater determinant of the *N* orbitals, the so-called Kohn–Sham orbitals, with the lowest eigenvalues E. It is relatively easy to unravel for these single-particle orbitals even for as many as a couple of hundred electrons [18]. The Kohn–Sham equations formally look considerably like self-consistent Hartree equations, the only difference being the presence of the exchange-correlation potential. This makes them much simpler to solve than the Hartree–Fock equations, in which the potential is orbital-dependent. In the Kohn–Sham and Hartree equations, the effective potential is the same for every orbital.

3.6 The Local Density Approximation

In band calculations, usually certain approximations for the exchange–correlation potential $V_{xc}(r)$ are used. The simplest and most frequently used is the local density approximation (LDA), where $\rho_{xc}(r, r'-r)$a form similar to that for a homogeneous electron has gas, but with the density at every point of the space replaced by the local value of the charge density, $\rho(r)$for the actual system:

$$\rho_{xc}(r, r'-r) = \rho(r) \int_0^2 d\lambda g_0\big(r - r' \vee, \lambda, \rho(r)\big) - 1, \tag{2.1.26}$$

Where, g_0 is the pair correlation function of a homogeneous electron system. Substituting (2.1.26) into (2.1.27) we obtain the local density approximation [44]:

$$E_{xc}[\rho] = \int \rho(r)\varepsilon_{xc}(\rho)\, dr, \tag{2.1.27}$$

Here, ε_{xc} is the contribution of exchange and correlation to the total energy (per electron) of a homogeneous interacting electron gas with the density $\rho(r)$. This approximationcorresponds to surrounding every electron by an exchange– correlation hole and must, as expected, be quite good when $\rho(r)$varies slowly. The DFT includes the exchange and correlation effects in a more natural way in comparison with Hartree-Fock-Slater method. Here, the exchange– correlation potential V_{xc} may be represented as

$$V_{xc}(r) = \beta(r_e)V_{GKS}(r), \tag{2.1.26}$$

where V_{GKS} is the Gaspar–Kohn–Sham potential, and r_e is given by

$$r_e(r) = \left[\frac{3}{4\pi}\rho(r)\right]^{1/3}. \tag{2.1.29}$$

This parameter corresponds, in order of magnitude, to the ratio of the potential energy of particles to their average kinetic energy

3.7 The Generalized Gradient approximation

An early endeavor to improve the LSDA was the inclination development estimation (GEA). Figuring for molecules and a jellium surface appeared, be that as it may, that the GEA doesn't improve the LSDA if the stomach muscle initio coefficients of the slope revision are utilized. The blunders in the GEA were examined by Langreth and Perdew and later by Perdew and colleagues. It was demonstrated that the second request developments of the trade and relationship openings in angles of the thickness are genuinely sensible near the electron, yet not far away. In the first work of Langreth and associates a summed up inclination guess (GGA) was developed by means of cut-off of the deceptive little wave-vector commitment to the Fourier change of the second request thickness angle extension for the trade relationship opening around an electron. Later Perdew and associates contended that the inclination developments can be made increasingly practical by means of genuine space shorts picked to authorize careful properties regarded by zero-request or LSD terms however abused constantly request extensions: The trade gap is rarely positive, and incorporates to - 1, while the relationship opening coordinates to zero. Various GGA plans were created by Langreth and Mehl, Hu and Langreth (LMH), Becke, Engel and Vosko, and Perdew and collaborators (PW), the three best and well known ones are those by Becke (B88),

Perdew and Wang (PW91), and Perdew, Burke, and Ernzerhof (PBE). In GGA the trade relationship utilitarian of the electron turn densities $\rho_{\uparrow}$ and $\rho_{\downarrow}$ takes the form

$$E_{xc}^{GGA}[\rho_{\uparrow}, \rho_{\downarrow}] = \int \quad d^3r\, f(\rho_{\uparrow}, \rho_{\downarrow}, \nabla\rho_{\uparrow}, \nabla\rho_{\downarrow}) \tag{2.1.30}$$

The GGA functionals were tried in a few cases, and were found to give improved outcomes for the ground-state properties. For iotas it was discovered that both all out energies and expulsion energies are improved in the LMH practical contrasted and the LSDA. The PW practical gives a further improvement in the all out vitality of iotas. The coupling energies of the first push diatomic atoms are additionally improved by both functional. In an investigation of the band structure of V and Cu, Norman and Koelling found that the LMH potential gave an improvement in the Fermi surface for V yet not for Cu. The strong vitality, the cross section parameters, and the mass modulus of third-push components have been determined utilizing the LMH, PW, and the angle extension functional in. The PW practical was found to give to some degree preferred outcomes over the LMH utilitarian and both were found to commonly evacuate a large portion of the mistakes in the LSD estimate, while the GEA gives more terrible outcomes than neighborhood thickness guess. For Fe GGA functional accurately anticipates a ferromagnetic bcc ground state, while the LSDA and the angle extension foresees a nonmagnetic FCC ground state. Likewise, the GGA amends LSDA underestimation of the cross section constants of Li and Na. Enormous number of test estimations demonstrated that GGA functional yield incredible improvement over LSD in the portrayal of finite frameworks: they improve the complete energies of particles and the strong vitality, harmony separation, and vibrational recurrence of atoms, however have blended history of achievements and disappointments for solids. This might be on the grounds that the trade connection opening can have a diffuse tail in a strong, yet not in a particle or little atom, where the thickness itself is all around confined. The general pattern is that the GGA thinks little of the mass modulus and zone focus transverse optical phonon recurrence, remedies the coupling vitality, and amends or overcorrects, particularly for semiconductor frameworks, the cross section consistent contrasted with LDA. The GGA doesn't take care of the issues experienced in the change metal monoxides FeO, CoO, and NiO. The attractive minutes and band structures acquired with the GGA for the oxides are basically indistinguishable off base ones from got with the LSDA. As of late, various endeavors have been made to

broaden the GGA by including higher request terms, specifically the Laplacian of the electron thickness, into the extension of the trade connection gap. Be that as it may, no broad trials of the nature of these new possibilities with application to solids have yet been made [19].

3.8 Pseudo-potentials

The key thought of "pseudo-potential" is the supplanting of one issue with another. The essential application in electronic structure is to supplant the solid Coulomb capability of the core and the impacts of the firmly bound center electrons by a powerful ionic potential following up on the valence electrons. Pseudo-potential can be created in a nuclear estimation and afterward used to process properties of valence electrons in atoms or solids, since the center states remain practically unaltered. Moreover, the way that pseudo-potentials are not special permits the opportunity to pick shapes that disentangle the computations and the translation of the subsequent electronic structure. The approach of "stomach muscle initio standard saving" and "ultra-soft" pseudo-potentials has prompted precise estimations that are the reason for a great part of the momentum innovative work of new techniques in electronic structure, as portrayed in the accompanying sections. A large number of the thoughts started in the orthogonalized plane wave (OPW) approach that throws the eigenvalue issue as far as a smooth piece of the valence capacities in addition to center (or center like) capacities. The OPW technique has been brought into the advanced system of all out vitality functional by the projector increased wave (PAW) approach that utilizations pseudo-potential administrators yet keeps the full center wave functions.

Norm-conserving pseudo-potentials

Pseudo-potentials generated by calculations on atoms (or atomic-like states) are termed "ab initio" because they are not fitted to experiment. The concept of "norm-conservation" has a special place in the development of ab initio pseudo-potentials; at one stroke it simplifies the application of the pseudo-potentials and it makes them more accurate and transferable. Norm-conserving pseudo-functions $\psi_{ij}(r)$ are normalized and are solutions of a model potential chosen to reproduce the valence properties of an all electron calculation. In the application of the pseudopotential to

complex systems, such as molecules, clusters, solids, etc., the valence pseudo-functions satisfy the usual orthonormality conditions as

$$\langle \psi_i^{\sigma,PS} \vee \psi_i^{\sigma',PS} \rangle = \delta_{i,j}\delta_{\sigma,\sigma'} \tag{2.1.31}$$

so that for the Kohn-Sham equations have the same form as

$$\left(H_{KS}^{\sigma,PS} - e_i^{\sigma}\right)\psi_i^{\sigma,PS}(r) = 0 \tag{2.1.32}$$

Ultra-soft pseudo-potential (USPP)

One goal of pseudo-potentials is to create pseudo-functions that are as "smooth" as possible, and yet are accurate. "Norm-conserving" pseudo-potentials achieve the goal of accuracy, usually at some sacrifice of "smoothness."

A different approach known as "ultra-soft pseudo-potentials" reaches the goal of accurate calculations by a transformation that re-expresses the problem in terms of a smooth function and an auxiliary function around each ion core that represents the rapidly varying part of the density. We will focus upon examples of states that present the greatest difficulties in the creation of accurate, smooth pseudo-functions: valence states at the beginning of an atomic shell, *Is,2p, 3d,* etc.

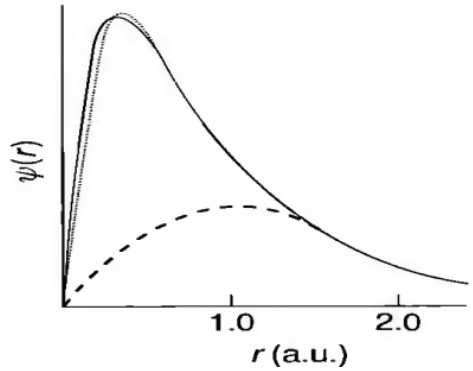

Figure 3.3: 2p radial wave function ψ(r) for oxygen treated in the LDA, comparing the all-electron function (solid line), a pseudofunction generated using the Hamann approach (dotted line), and the smooth part of the pseudofunctionΦ in the "ultrasoft" method (dashed line) [57]

For these states, the OPW transformation has no effect since there are no core states of the same angular momentum. Thus, the wave functions are needless and extend into the core region. Accurate representation by norm-conserving pseudo-functions requires that they are at best only moderately smoother than the all-electron function (see Fig.2.3) The difference in the norm equation $Q_l = \int_0^{R_c} dr\phi_l(r)^2$from that norm-conserving function $\phi = r\Phi$ (either an all-electron function or a pseudofunction) is given by

$$\Delta Q_{s,s'} = \int_0^{R_c} dr \Delta Q_{s,s'}(r). \tag{2.1.33}$$

Where

$$\Delta Q_{s,s'}(r) = \phi_s\ (r)\phi_{s'}(r) - \Phi_s\ (r)\Phi_{s'}(r). \tag{2.1.34}$$

A new non-local potential that operates on the $y can now be defined to be

$$\delta\hat{V}_{NL}^{US} = \sum_{s,s'} D_{s,s'} \vee \beta_s > \beta_{s'} \vee, \tag{2.1.35}$$

Where

$$D_{s,s'} = B_{s,s'}\varepsilon_{s'}\Delta Q_{s,s'}. \tag{2.1.36}$$

For each reference atomic states *s*, it is straightforward to show that the smooth functions

$\Phi_s$are the solutions of the *generalized eigenvalue problem*

$$\left[\hat{H} - \varepsilon_s\hat{S}\right]\Phi_s = 0, \tag{2.1.37}$$

With$\hat{H} = \frac{-1}{2}\Delta^2 + V_{local} + \delta\hat{V}_{NL}^{US}$ and $\hat{S}$ an overlap operator,

$$\hat{S} = \hat{1} + \sum_{s,s'} \Delta Q_{s,s'} |\beta_s > \beta_{s'}|, \tag{2.1.38}$$

which is different from unity only inside the core radius. The eigenvalues ε_s agree with the

All-electron calculation at as many energies s as desired. The full density can be constructed from the functions$\Delta Q_{s,s'}(r)$, which can be replaced by a smooth version of the all-electron

density. The advantage of relaxing the norm-conservation condition $\Delta Q_{s,s'} = 0$ is that each smooth pseudofunction ϕ_s can be formed independently, with only the constraint of matching the value of the functions $\phi_s(R_c) = \psi_s(R_c)$ at the radiusR_c. Thus, it becomes possible to choose R_c much larger than for a norm-conserving pseudopotential, while maintaining the desire accuracy by adding the auxiliary functions $\Delta Q_{s,s'}(r)$ and the overlap operator S. An example of the un-normalized smooth function for the 2p state of oxygen is shown in Fig. 2.9.1, compared to a much more rapidly varying norm-conserving function [20]

3.9 Band Structure

If we knew the potential$V_P(r)$, and could solve the one-electron Schrödinger equation

$$(\frac{-\hbar^2}{2m_e}\nabla^2\psi(r) + V_P(r)\psi(r) = E\psi(r)$$

we could ascertain the energies E of the entirety of the different potential states. There are a few different ways of moving toward such figuring from first standards, and we won't go into those here. The after effects of such counts give what is known as a band structure. The electronic conditions of precious stones are portrayed by the band hypothesis of solids. The external orbital's of the molecules in a thickly stuffed strong cover with one another as the synthetic bonds that hold the gem together are framed. This causes the discrete vitality levels of the free ion as to be expanded into groups. The differentiation between a protector and a semiconductor is identified with the size of the band gap. Semiconductors have littler band holes than encasings. The free electrons in the conduction band can direct power effectively in a similar way as the free electrons in metals. Semiconductors, hence, have a higher conductivity than encasings, yet a littler conductivity than metals as a result of the modest number of free electrons [21]. There are various groups in a band structure (in actuality a limitless number), yet generally, just a couple are significant in deciding specific properties of a material. Fig. 8.4 outlines a basic band structure. Each band has an all outnumber of permitted k-states equivalent to the number of unit cells in the precious crystal.

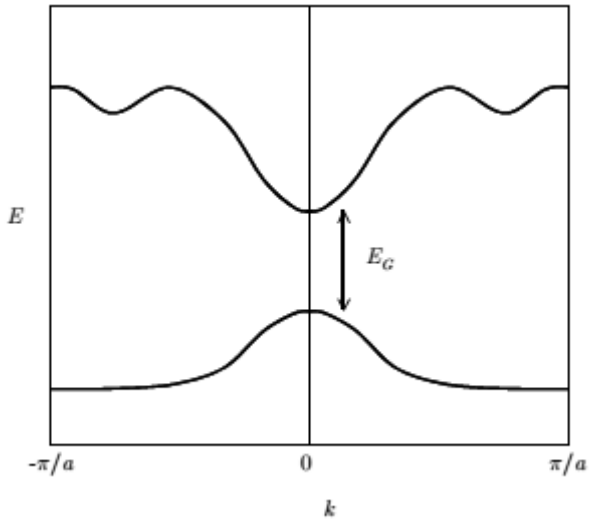

Fig. 3.4: Figurative illustration of a semiconductor band structure, plotted along one crystal direction. The upper "band" (line) will be essentially empty of electrons, and is called the conduction band; the lower band will be essentially full of electrons, and is called the valence band [58]

Fig. 2.4 illustrates a simplified band structure. In each band, we only have to plot *k*-values from $-\pi$ / a to π / a. The band structure in Fig. 2.4 is also drawn to be symmetric about $k = 0$. Band structures are often symmetric in this way. In our simple one-electron model, neglecting magnetic effects, the existence of symmetries like this is easily proved [22].

3.10 GW approximation

While we have given some justifications to utilizing a straight forward LSDA band structure way to deal with assessing excitation energies, various materials with intriguing attractive properties include firmly corresponded electronic states, and other estimated approaches have been created to go past the LSDA. For the quasi-particle issue, the focal issue is a sufficient estimation for the self-vitality administrator, $\Sigma_{GW}(r, r'; E)$. A working technique for tackling this issue is the purported GW estimation. On the off chance that the pinnacle is sufficiently sharp, well-defined quasi-particle vitality can be acquired. Where the self-energy is

$$\Sigma_{GW}(r, r'; t) = iG(r, r'; t)W(r, r': t) \qquad (2.1.39)$$

The self-vitality in the GW A has a similar structure as that in the Hartree-Fock estimate aside from that it relies upon the vitality and contains a term that relies upon abandoned states as an outcome of relationship impacts. In this manner, the GW A can be deciphered as a speculation of the Hartree-Fock estimate with a potential that contains dynamical screening of the Coulomb potential. The GWA has been fruitful in treating the quasi-particle frameworks, for example, free-electron like metals and semiconductors It can be demonstrated that the GWA hypotheses might be identified with a Hartree-Fock hypothesis with a recurrence and orbital-subordinate screened Coulomb association and, at any rate for confined states, for example, d or f orbital's of progress metal or uncommon earth metal particles [23].

CHAPTER 4

METHODOLOGY

4.1 General Consideration

In this chapter, we discuss details about our present work with the first principle pseudo-potential-based density functional calculations including norm-conserving pseudo-potential in the DFT approach by using The quantum ESPRESSO (QE) computational package. Some practicable commands along with their functions are well detailed here.

4.2 Quantum Espresso Program

In this activity, you will use the Density Functional Theory (DFT) to investigate the properties of different materials. DFT is broadly utilized in industry, and in the scholastic research network since it is one of the computational techniques that can (roughly) tackle reasonable quantum mechanical issues numerically [24]. Quantum ESPRESSO-a condensing for Quantum Open-Source Package for Research in Electronic Structure, Simulation, and Optimization program is a multi-reason and multi-stage PC coding program for electronic-structure figuring and materials demonstrating. This bundle is essentially utilized in the stomach muscle ab-initio estimations of dense issue frameworks. In a controlled issue material science, its ordinary application in the stomach muscle ab-initio estimations like-basic advancements (both at zero and limited temperature), direct reaction computations (Phonons, flexible constants, dielectric, and some more) and so forth stretches out to high-temperature atomic elements. The significant element of the bundle remembered for the product are :

- Plane Wave self-consistent field (PWscf)
- First-Principles Molecular Dynamics (FPMD) and
- Car-Parrinello (CP). QE, based on DFT, implements a variety of methods and algorithms for a chemically realistic modeling of materials from the Nano-scale upwards

- Chemical reactivity and transition-path sampling, using Nudged Elastic Band (NEB) method
- Computational microscopy (STM). This package uses a plane waves (PWs) basis set for the expansion of electronic wave function, a pseudo-potentials (PPs) to represent electron-ion interactions and DFT for the description of electron-electron interaction.

Some basic computations/simulations that can be performed by this package include:

- Calculations of the Kohn-Sham (KS) orbitals and energies for isolated and extended systems, and of their ground states energies.
- Structural modeling (equilibrium structures of molecules, crystals, surfaces).
- Atomic forces and stresses.
- Ground state studies of magnetic or spin-polarized systems.
- Dynamical modeling (first-principles molecular dynamics) either in the electronic ground state (Born-Oppenheimer) or with fictitious electronic kinetic energy (Car-Parrinello).

Density-Functional Perturbation Theory (DFPT) used in the package to calculate the energy derivatives and related quantities. QE package are used as our first — principles code. QE is a full ab- initio package implementing electronic structure and energy calculation, linear response method (to calculate dielectric constants, Born effective charge and phonon dispersion curves) and third order an-harmonic perturbation theory. It also contains two molecular- dynamics codes, CPMD (Car-Parrinello Molecular Dynamics) and FPMD (First-Principles Molecular Dynamics). Among them, to perform the total energy calculations, PWscf code is used, which used both norm-conserving pseudo-potential (PP) and Ultra soft Pseudo-potentials (US-PP) within DFT. In our case, we use Quantum ESPRESSO integrated module of codes, based on DFT by using plane basis set for expansion of wave function and pseudo-potential with required content in first-principle method of calculation to calculate total energies and optimize geometries of transition metal Fe and Ni. Also, by using this package, band structure is calculated and partial density of states (PDOS) is used to find the nature of material.

4.2.1 PWscf

PWscf stands for Plane Wave self-consistent field (which in earlier releases included Phonon and PostProc), developed by Stefano Baroni, Stefano de Gironcoli, Andrea Dal Corso (SISSA) Paolo Giannozzi (Univ. Udine), and many others [25]. PWscf implements an iterative approach for self-consistency, in the framework of the plane-wave pseudo potential method. This package uses the well-established LDA and GGA exchange-correlation functional, including spin-polarizations. The main feature of PWscf calculation is the self-consistency calculations, structural relaxation, electronic structure calculations, variable cell molecular dynamics calculation etc. performed by invoking executable file called pw.x. The structural optimization is performed using the Broyden-Fletcher-Goldfarb-Shanno (BFGS) [42]

Some of the most important parameters in the input file of the Quantum espresso are as indicated below.

- &CONTROL: general variables controlling the run
- &SYSTEM: structural information on the system under investigation and
- &ELECTRONS: electronic variables: self-consistency, smearing
- ibrav : 2, this keyword generates face centered cubic (fcc) structure.
- celldm(1): specifies the lattice constant of the crystal and are usually given in atomic unit.
- ecutwfc: kinetic energy cutoff (Ry) for wave functions (1 Ry=13.6ev).
- nat: number of atoms in the unit cell which is 1.
- ntyp: number of types of atoms in the unit cell.
- nbnd: represents the number of electronic stated (bands) to be calculated.
- Atomic Species: It specifies the symbols of the atoms, their corresponding masses (in amu) and the name of the files containing the pseudo-potentials.
- Atomic Positions: specifies the atomic co-ordinates of the atoms which are defined for the proper structure.
- K-points: represents the rectangular grid of points of dimensions, spaced evenly throughout the Brillouin zone and this keyword requires appropriate unit.

4.2.2 Post Processing

The package called Post processing was Originally developed by Stefano Baroni, Stefano de Gironcoli, Andrea Dal Corso (SISSA), Paolo Giannozzi (Univ. Udine), and many others. After the Self Consistent calculation has been converged, we use many small calculations such as plotting of band, density of states (DOS) etc.

The main post processing codes which extract the specified data/files from the PWscf calculations and perform further calculations are as follows;

- pw.x: We use this command to run the input files of scf and nscf calculations of energy and wave functions at each k-points, which extracts the output files for the energy calculation at every k-points.
- bands.x : This extracts the files from PWscf calculation and records its eigenvalues at different K-points with corresponding energies values ready for further processing. The code bands.x also performs the symmetry analysis of the band structure.
- plotband.x : The output file of bands.x is directly read and converted to plottable format by auxiliary code plotband.x. The value of k-points must be correctly put in a sequence, otherwise unpredictable plots may result if k-points are not in sequence along lines or if two consecutive points are same. Thus, proper choice of sequence of k-points is important.
- dos.x : This code helps us to calculate the electronic density of states at different k-points. • projwfc.x : This code calculates projections of wave functions over atomic orbitals. It gives the contributions of the atomic orbitals s, p, d, f.

CHAPTER 5

RESULTS AND CONSIDERATION

5.1 General Consideration

This thesis has describes the comparative study of element iron (Fe) and nickel (Ni). One of the main challenges in first principle calculation is the geometric optimization of structures. We have taken out the energy minimization of Fe and Ni, followed by the study of electronic band structures and the density of states. The calculation has been carried out using density functional theory using generalized gradient approximation. At first, in the GGA method, energy minimization is done with respect to the lattice parameter then the same lattice parameter corresponding to the minimum energy state is used to carry out further calculations. In-band structure calculations, We plotted the graph of energy versus the high symmetry k-points and then analyzed the properties of the substance on the basis of band lines and band gap. To view the individual contribution of different orbital electrons, we study the conduction band edge and valance band edge. Likewise, the Density of states (DOS) is performed to get information about the nature of the band gap and the Partial Density of states (PDOS) gives information about the origin of bands. In all these self-consistent fields (SCF) calculations, we have used the convergence criteria as the difference between energy in the order of 10^6 Rydberg.

In this chapter, we discuss about:

- Calculation of lattice parameter.
- Calculation of Density of states (DOS) as well as Partial Density of States (PDOS) and plotting.

Then we have performed the series of following convergence tests and energy minimization:

5.2 Structural Optimization:

We carried out the self- consistent field (scf) calculations to determine basic parameters:

kinetic energy cut-off for the plane wave basis and k-points grid by testing the convergence of total energy with these parameters individually and calculation of lattice parameter by energy minimization.

5.2.1 Kinetic Energy cut-off (ecutwfc)

The plane wave scf code implemented in the Quantum Espresso expands the electron wave-function in terms of the infinite basis function that are plane waves. The value of the kinetic energy cut-off corresponds to the neighboring interactions in the periodic system. If we take this cut-off energy large, we include long range interactions and the results will be more accurate, but this takes more computing resources. If we take this energy small, the results could be inaccurate though computationally cheap. Therefore, we have to take optimum value of this cut-off energy. It is expressed in unit of the energy Ry. The plane wave expansion in the reciprocal space is

$$\psi_k(r) = \frac{1}{\Omega}\sum_G C_{k.G} e^{i(k+G).r} \tag{4.1}$$

where Ω is the volume of the box, G are the reciprocal lattice vectors defined by $G.l = 2\pi m$ for all l, where l is a lattice vector of the crystal and m is an integer, $C_{k.G}$ are the coefficients for the plane waves and k represent the reciprocal space vectors within the first Brillouin zone of the periodic cell.

In principle, we need infinite numbers of plane waves but in order to reduce the computational cost we have to truncate the plane wave expansion from some acceptable value. To make the plane wave expansion (5.1) finite, we truncated according to the condition.

$$\frac{|k+G|^2}{2m} \leq E_{cut} \tag{4.2}$$

We performed the scf calculations using the experimental value of the lattice parameter (a=5.4168 Bohr) and some arbitrary k-point mesh in the scf input file for Fe. The scf calculations were performed for different values of the ecutwfc ranging from 40 Ry to 120 Ry. At these different values of cut-off energy, we found different values of total scf energy. Then we plot the graph between the scf total energy versus kinetic energy cut-off value and the appropriate value of kinetic energy cut-off is chosen from which the convergence of total energy starts to occur. In the case of Iron, it is found to be 95 Ry, which is shown in the Fig. (5.1). So, for further calculations,

the value of ecutwfc = 95 Ry is appropriate to use for Iron. In our case, the pseudo-potential used is PredewBerke-Erzndof (PBE) pseud o-potentials generated using "atomic" code by A. Dal Corso (espresso distribution).

When a graph was plotted for the relationship between cut-off energy along X-axis versus total energy along Y-axis of Fe, following graph was obtained.

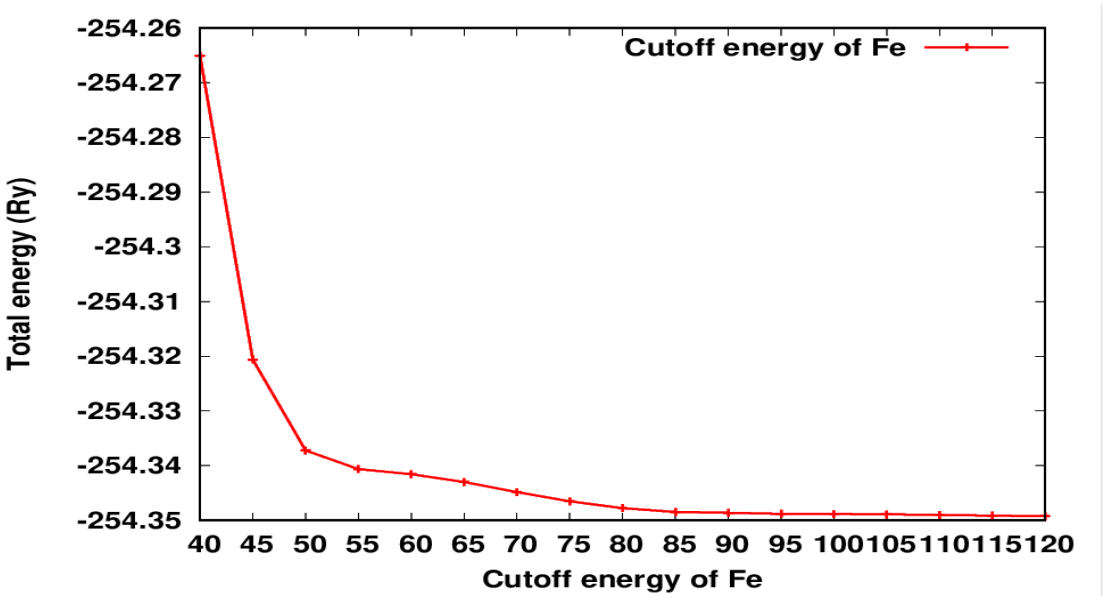

Figure 5.1: The plot of Total energy with cut-off energy of Fe

To determine the value of kinetic energy cut-off we performed the scf calculation using lattice parameter a=6.659 from literature and some arbitrary k-point mess (8, 8, 8) in scf input file for Ni. Similarly we perform same ecutwfc range as Fe in this case and we get different values of total energy in self-consistent field. Then plot of total energy versus kinetic energy cut-off value for FCC structure of Ni is shown in Figure (5.2). Clear from the Fig. (5.2) that there is nominal variation in total energy above 95 Ry. Therefore in the rest of calculations, our cut-off energy is 95 Ry.

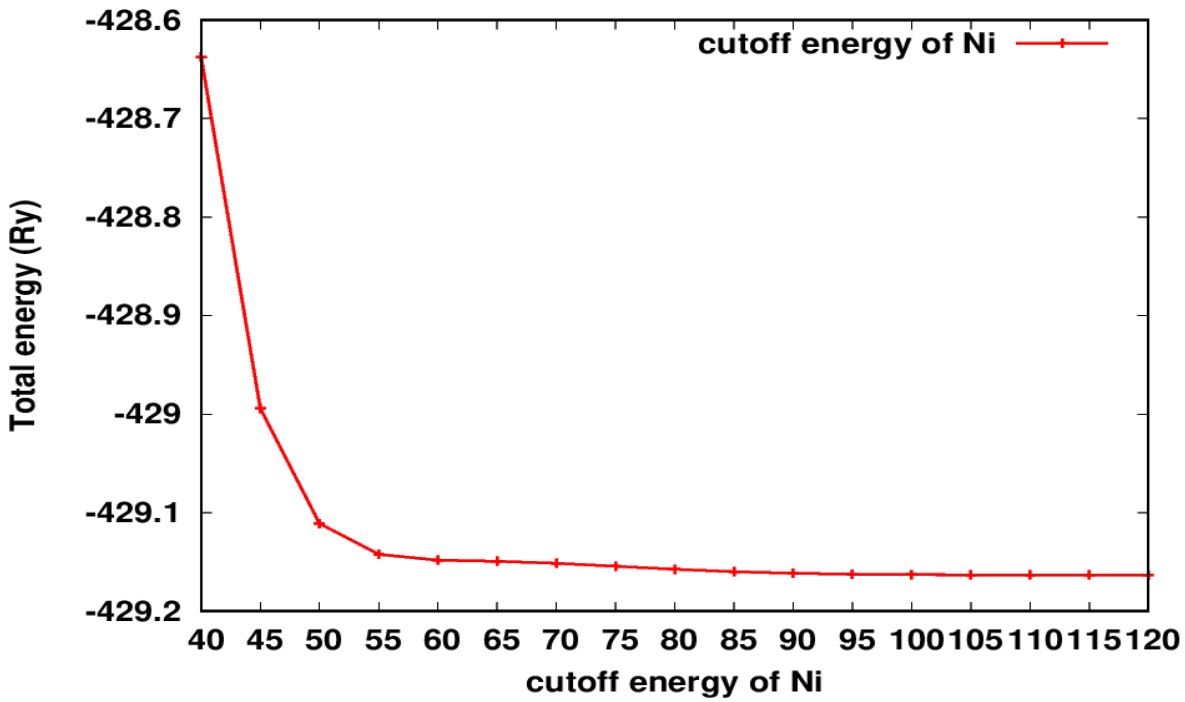

Figure 5.2: The plot of Total energy with cut-off energy of Ni

5.2.2 Lattice Parameter

Lattice constant is a property of crystal lattice i.e. periodic arrangement of atoms in three dimensions whether it is not a property of atoms. Basically, the lattice constant is the length of periodicity of the lattice repeats itself, for most crystals the lattice constant are few angstroms. After the calculation and value of ecutwfc and, we performed a convergence test for lattice parameter by using the converged value of ecutwfc for both Fe and Ni. For Fe, we performed the scf calculations for total scf energy with different value of lattice parameters ranging from 5.02 to 5.82 Bohrs to optimizing lattice parameter by using optimized value of ecutwfc. Then we plot a graph between total energy with lattice parameter which is shown in Fig. 5.3

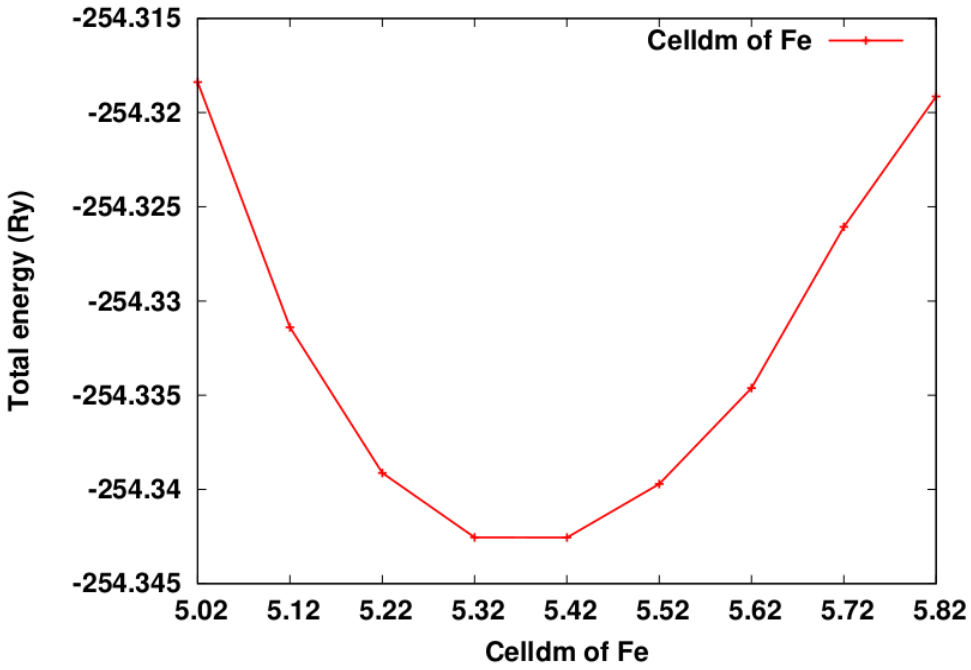

Figure 5.3: The plot of Total energy with lattice parameter of Fe

At different value of lattice parameter we found different value of total energy. Then, we obtained the suitable value of parameters for the input file at which the total energy is minimum. From Fig. 5.3, the appropriate value of lattice parameter is at which the minimum total energy is at 5.42 Bohr. The experimental value of lattice parameter is5.4168 Bohr which is closer to our calculate value of lattice parameter and we get 0.05%error from previous work [27].

For Ni, we performed the scf calculations for total scf energy with different value of lattice parameters ranging from 6.26 to 7.16 Bohr by using optimized ecutwfc.

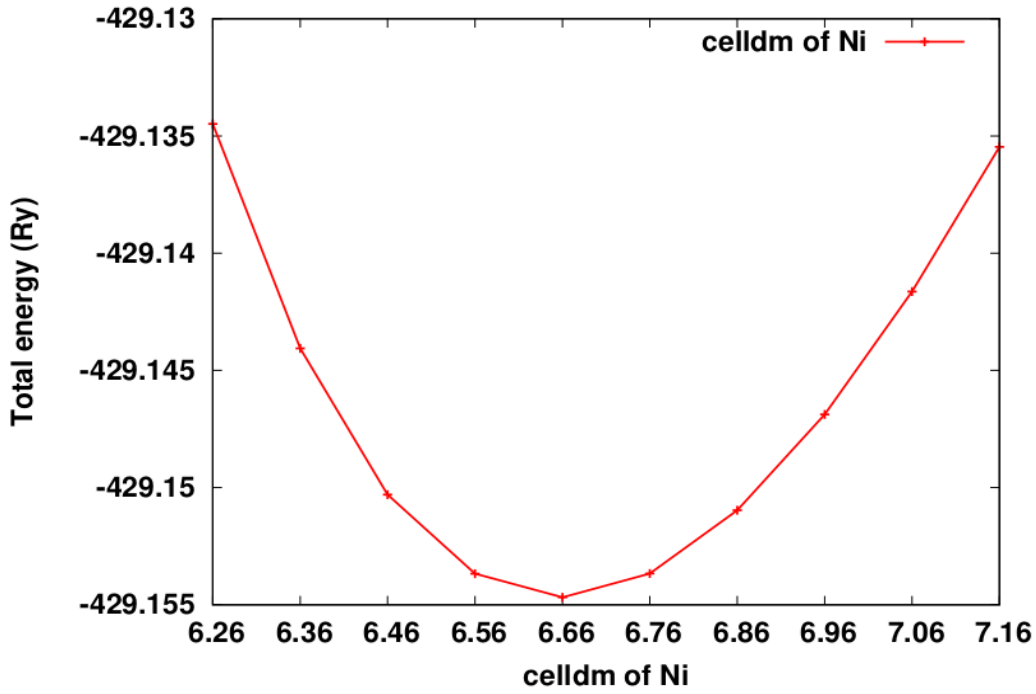

Figure 5.4: The plot of Total energy with lattice parameter of Ni

Then, we obtained the suitable value of parameters for the input file at which the total energy is minimum. From Fig. 5.4, the minimum total energy is at 6.66 Bohr. The experimental value of lattice parameter is6.659 Bohr which is closer to our calculate value of lattice parameter and we get 0.0152% from previous work [29].

5.2.3 k-point grid

In order to perform the Brillouin zone interaction in discrete scheme, it is essential to have a large number of grid points. But in practice, due to limitations of computational resources, we optimize the number of k-points grids. By calculating total energy versus k-point grids the rectangular grid of points of dimensions Kx×Ky×Kz, spaced evenly throughout the Brillouin zone is called k-points grid. More the number of the grid points sampling will be more finer and accurate but computationally expensive. Here, the size of grid required depends on the system under study. We can estimate appropriate size by means of total energy calculation. Our approach of k-point sampling is as suggested by Monkhrost and Pack [26]. At first, we performed the scf calculations of Fe for total scf energy with different values of k-points grid starting from 2×2×2 to 18×18×18. The calculated data of k-point grid vs its corresponding total scf energy is shown in Fig. 5.5.

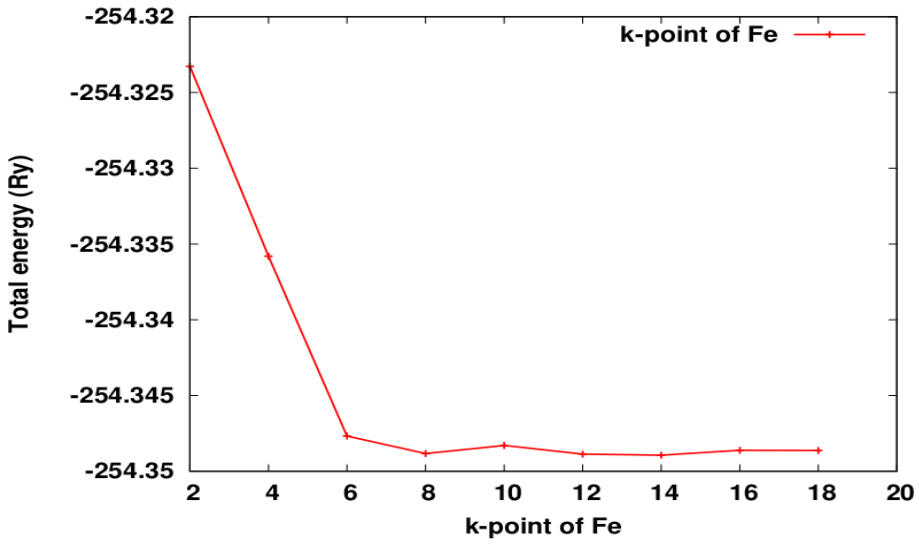

Figure 5.5: The plot of Total energy with k-point grid of Fe

From Fig.5.5 it is clearly seen that total energy of Fe remains almost constant from the k-point grid 8×8×8. So, it is appropriate to use the value of k-point grid as 8×8×8 for our further calculation. Then we performed the scf calculations of Ni for total scf energy with different values of k-points grid starting from 2×2×2 to 18×18×18. The calculated data of k-point grid vs its corresponding total scf energy is shown in Fig. 5.6.

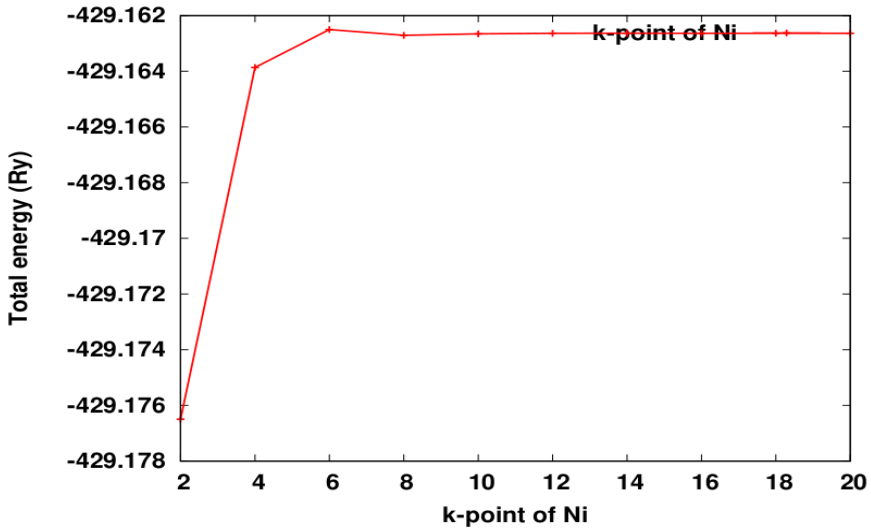

Figure 5.6: The plot Total energy with k-point grid of Ni

From Fig. 5.6, it is clearly seen that total energy remains almost constant from the k-point grid 6×6×6. So, it is appropriate to use the value of k-point grid as 6×6×6 for our further calculation.

5.2.4 Degauss

In the case of degauss you should use the smallest value at which your calculation does not struggle to converge. After optimization of all Structure of Fe and Ni, we are intended to study the effect of degauss on elements. To account the degauss, we have taken all optimized value and apply degauss in the range of 0.01 to 0.1. Then we plotted a graph between degauss value vs. total kinetic energy which is shown in Figure 5.7 and figure 5.8 for Fe and Ni respectively. From the graph it is observed that degauss is constant to 0.02 so further calculation take place by using degauss 0.02.

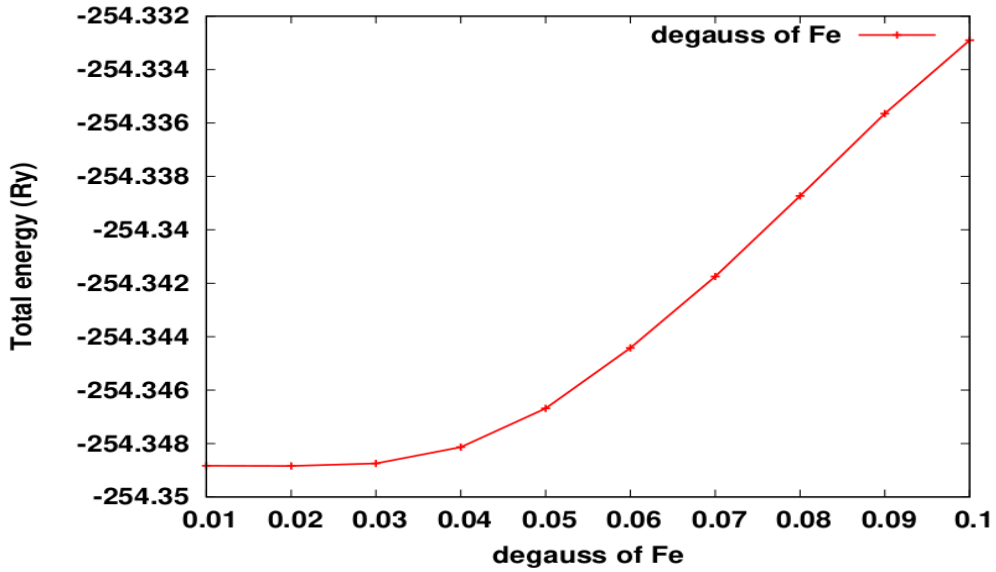

Figure 5.7: The plot of Total energy with degauss of Fe

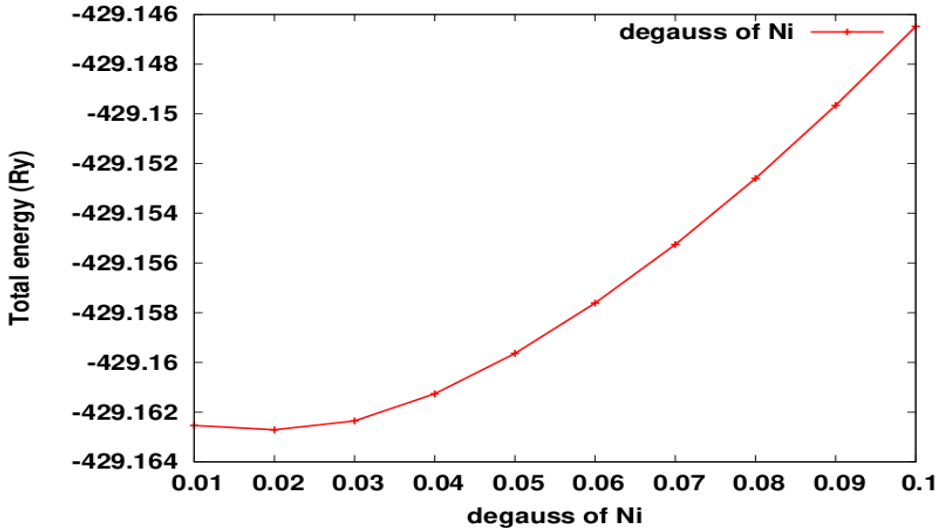

Figure 5.8: The plot of Total energy with degauss of Ni

We have also calculated the band structure of Transition Metal Fe and Ni. For other calculations of Fe and Ni, we took (8×8×8) and (6×6×6) respectively k-points along specific direction of irreducible Brillouin zone in order to obtain fine band structure which is performed by executable pw.x. Then, we performed post processing calculations with executable plotband.x in order to obtain band structure of Iron(Fe) and Nickel(Ni). Further, we have calculated the DOS and PDOS for both Fe and Ni structure. Finally we performed scf calculation and then nscf calculation; we used denser k-point mesh in order to obtain smooth partial density of states curve. These calculations were performed using the executable pw.x. Then, we performed PDOS calculation using executable projwfc.x command. In this section, we discussed the results of the first principles calculations carried out to obtain: Band structure calculation of Fe and Ni, Density of states of structure of Fe and Ni and Partial Density of states of structure of Fe and Ni

5.3 Band structure

In the first principles electronic structure calculation of crystals, the electronic band structure is one of the most widely applied analytical tools especially within the Kohnsham framework of density functional theory. The band structures of solid are helpful to determine different electronic properties of solid. It contains the basic ingredients to almost all the crystal properties. Since the atoms in a solid are closely packed the interaction between them perturbed the initial atomic levels when a large

number of atoms are brought together. Electrons in the orbitals are filled up according to Pauli's exclusion principle i.e. no two electrons can occupy the same energy state. A band constitutes a sort of energy continuum, in which separate level due to individual atoms cannot be identified. In the process of inter atomic interaction, the inner shell electron stated are the least affected. Whereas the valance electron, which are closest to neighboring ions, are the most affected. The effect of bringing one atom closer to the other is to split a single sharp level. The bands structures of solids are helpful in determining different electronic and optical properties of the solid.

The band structure is calculated by pseudo potential and plane wave basis set method within the Density functional theory (DFT), treating exchange- correlation functional with generalized gradient approximation (GGA) in the form of PredewBerke- Erzndof (PBE) functional. All pseudo potential used in the calculations were norm- conserving scalar relativistic and full relativistic pseudo potentials. All calculation was performed within the Quantum- ESPRESSO package, plane wave kinetic energy cut-off were set at 95 Ry for Fe and Ni. We took uniform grid of k-vector (k-points) in X-Y plane ranging from 1 to 1 in the unit of 2π a. There is overlap of band in iron and nickel shows metallic character of iron and nickel.

The band structure calculation of Fe is shown in Fig. 5.9.

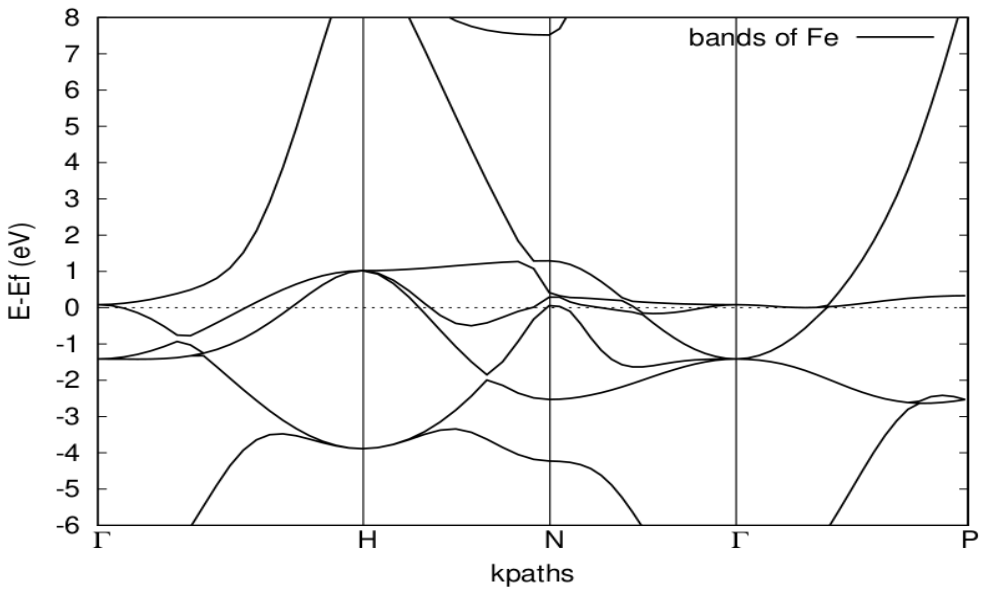

Figure 5.9: the plot of energy gap between conduction and valence band of Fe

The band structure calculation of Ni is shown in Fig. 5.10.

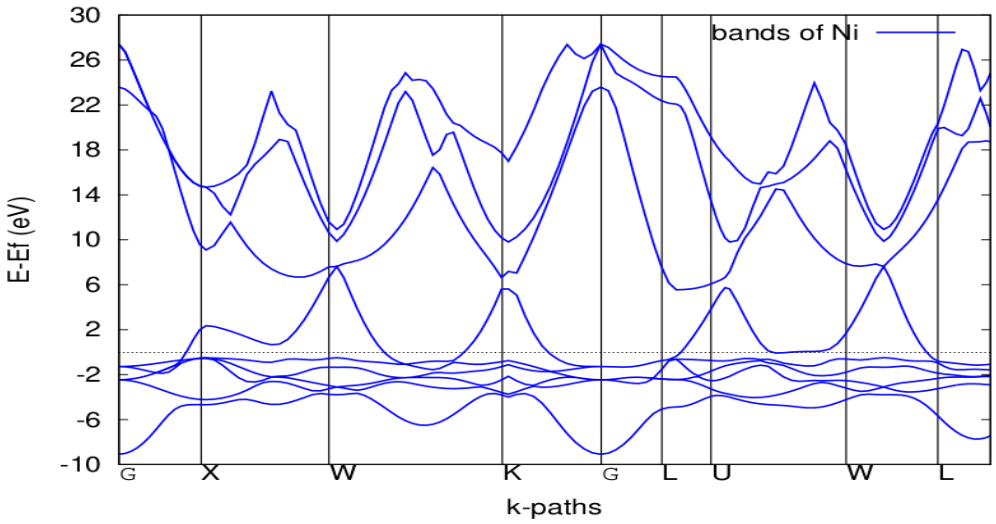

Figure 5.10: The plot of energy gap between conduction and valence band of Ni

5.4 Density of States

The density of states (DOS) is defined as the number of states per unit energy range available for the particles to be occupied. In other words, the density of states refers to the number of quantum states per unit energy range and it indicates how density packed quantum states in a particular system. In solid state and condense matter physics, the density of states is of immense important as it can be used to calculate the various parameters that give the insight of the different electronic, magnetic and transport properties. For example, Specific heat and paramagnetic susceptibility of a substance, mobility of charge carriers, diffusion properties and so on can be readily computed with the knowledge of density of states (DOS). Moreover, the density of states provides numerical information on the states that are available at each energy level. The value of zero density of states indicates that there are no available states for occupation in an energetic level

The density of sates is calculated by pseudo-potential and plane wave basis set method within the Density functional theory (DFT), treating exchange- correlation functional with generalized gradient approximation (GGA) in the form of PredewBerke- Erzndof (PBE) functional. All pseudo-potential used in the calculations were norm- conserving scalar relativistic and full relativistic pseudo-potentials. All calculation was performed within the Quantum- ESPRESSO package, plane wave kinetic energy cut-off was set

at 95 Ry for Fe and Ni. The smooth nature of graph shows iron and nickel can ionic bond.

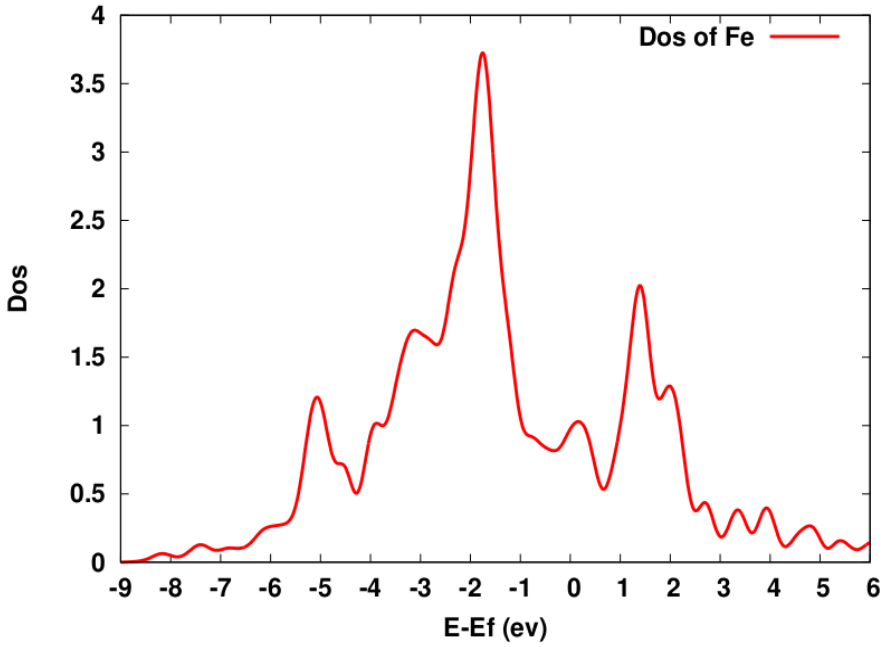

Figure 5.11: DOS curve of Fe with energies at DeltE=0.01

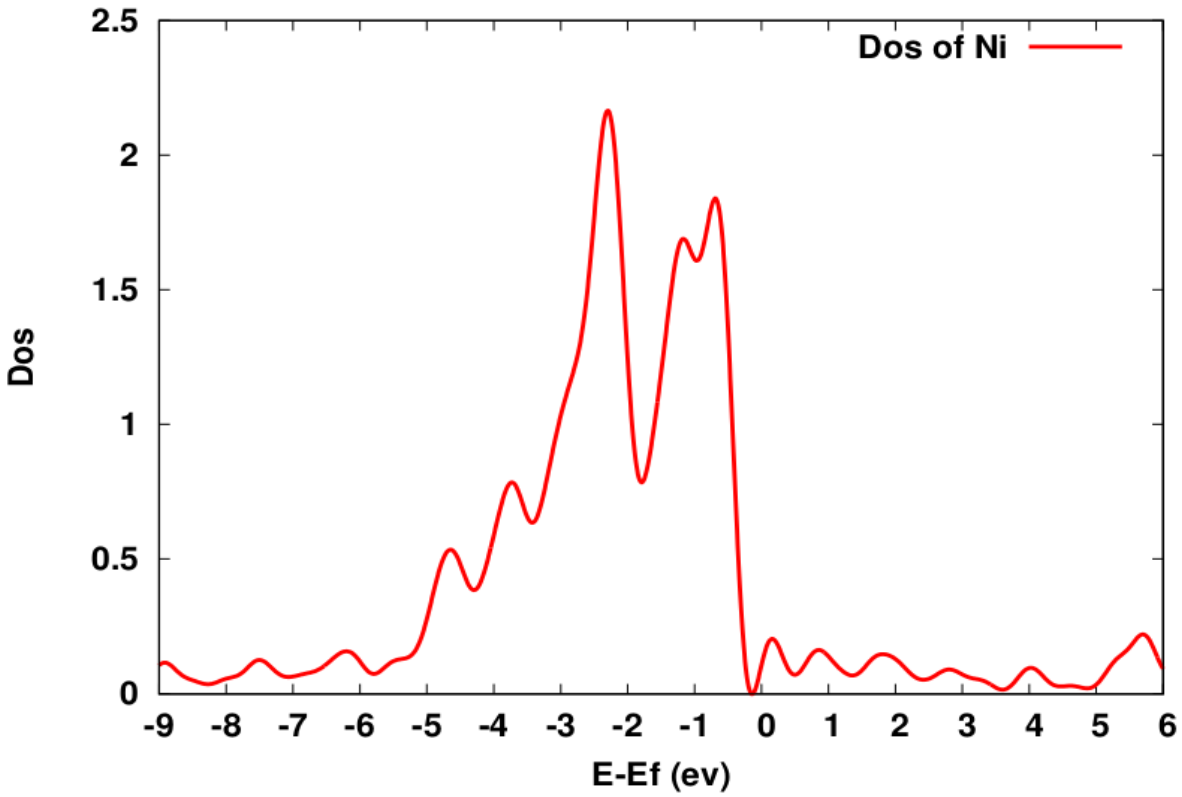

Figure 5.12: DOS curve of Ni with energies at DeltE=0.01

5.5 Partial Density of States

The results of partial densities of states (PDOS) of Fe and Ni help to further elaborate the nature of band gap as shown in Fig. 5.13 and Fig.5.14. The partial density of states gives information about the origin of bands and the graph shows transfer of electron from s orbital to p orbital.

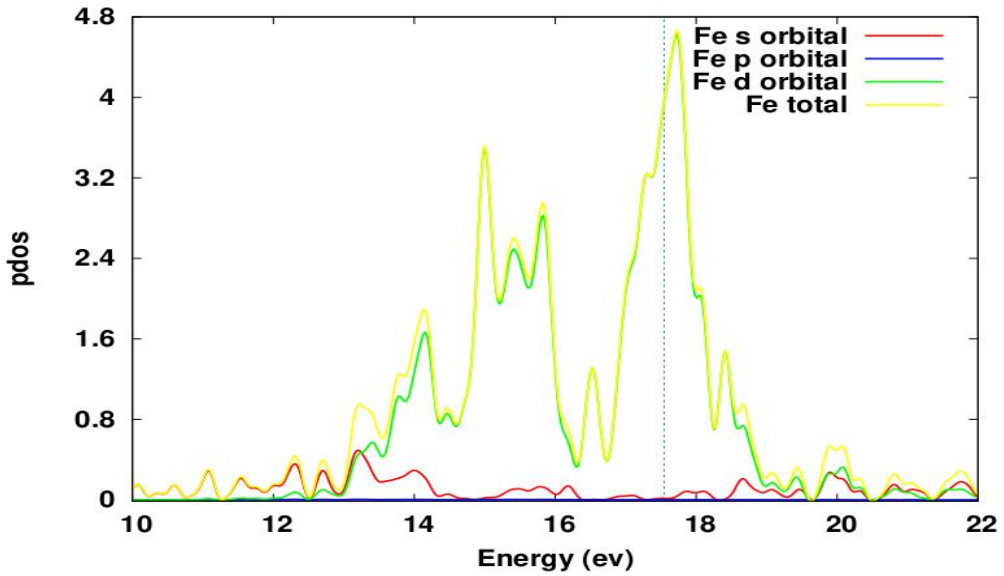

Figure 5.13: PDOS curve of Fe with energies at DeltE=0.01

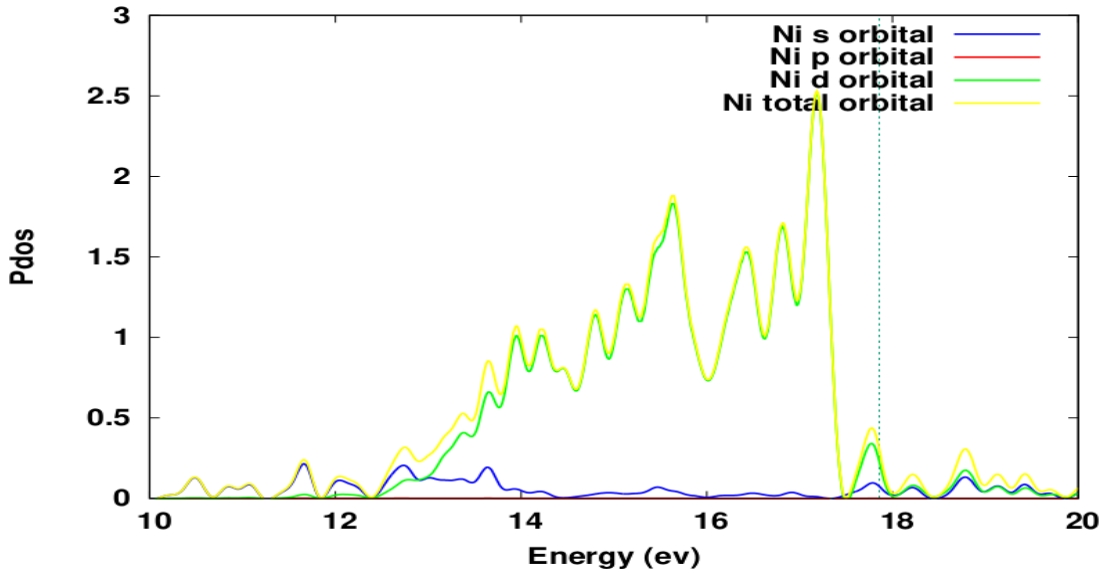

Figure 5.14 PDOS curve of Ni with energies at DeltE=0.01

CHAPTER 6

CONCLUSION AND CONCLUDING REMARKS:

This thesis has successfully employed to examine the structural properties of transition element Fe and Ni with the help of DFT, GGA, implemented with Quantum ESPRESSO code. At first we have constructed optimized structure of unit cell of BCC structure of Fe and FCC structure of Ni. During optimization, the kinetic energy cut-off energy is found to be 95 Ry having k-point grid (8×8×8) for Fe. Then we estimate the lattice Parameter is found to be 5.42 Bohr for Fe which is very near with experimental results as well as previous calculated data. Which is only 0.05% deviated from experimental result and previous data. Thus the lattice parameter of Fe estimated with GGA method is in close agreement with experimental values. Then we have study the band structure and found bands are overlap, density of states and partial density of states of Fe in which p-orbital have very less contribution in PDOS using GGA method in QE package.

Similarly, optimization, the kinetic energy cut-off energy is found to be 95 Ry having k-point grid (6×6×6) for Ni. Then we estimate the lattice Parameter is found to be 6.66 Bohr for Ni which is very near with experimental results as well as previous calculated data. Which is only 0.015% deviated from experimental result and previous data. Thus the lattice parameter of Ni estimated with GGA method is in close agreement with experimental values. Then we have study the band structure and found that bands are overlap, density of states and partial density of states of Ni in which p-orbital have very less contribution to PDOS by using GGA method in QE package.

This shows that Quantum ESPRESSO code using the plane-wave pseudo-potential method can be used to perform first-principles calculations to study the electronic and other system which is more complex of transition element. We believe code can be used to study correlated systems for interest to current research to amble technological potential they support. All our study method which we have performs in this work can be used standard frame work to calculate the electronic, magnetic, and structural properties of materials in the elements and other related materials for which experimental data are not available.

6.1 Further Enhancement

The unanswered question from this work are:

1. We can study optical, thermal expansion, magnetic properties, and phonon properties of Fe and Ni.
2. We also can study the effect of doping of other suitable atom with Fe and Ni.
3. We also study same from other different method suitable for these elements.

BIBLIOGRAPHY

[1] Robert H. Crabtree, *The Organometallic Chemistry of the Transition Metals* John Wiley & Sons, Inc., Hoboken, New Jersey (2014)

[2] J. R. Hook, H. E. Hall, *Solid state physics*, Wiley (1991)

[3] Harald Ibach, Hans L., *Solid-state physics an introduction to Principle of material science*, Springer Verlag Berlin Heidelberg, (2009)

[4] Richard J. D. Tilley - *Crystals and Crystal Structures*, Wiley (2006)

[5] Giuseppe Iadonisi, Giovanni Cantele, Maria Luisa Chiofalo, *Introduction to Solid State Physics and Crystalline Nanostructures*, Springer-Verlag Mailand, (2014)

[6] R.Murugeshan *Modern Physics* S. Chand, New Delhi (2009)

[7] Charles Kittel *Introduction to Solid State Physics*, Wiley (2005)

[8]J W Mullin *Crystallization*, Butterworth-Heinemann (2001)

[9] Ashcroft, Neil W, Mermin, David N - *Solid State Physics*

[10] https://periodictable.com/Elements/024/data.html (Retrived 25Aug 2020)

[11] Vishnu Swarup Mathur, Surendra Singh - *Concepts in Quantum Mechanics*- Chapman &Hall_CRC (2009)

[12] Philip A. Schweitzer, P. E**.** *METALLIC MATERIALS Physical, Mechanical, and Corrosion Properties*, New York Basel (2003)

[13] C. Leyens and M. Peters. *Titanium and titanium alloys fundamentals and applications*, Wiley VCH John Wiley (2003)

[14] Pergamon Materials Series 12] S. Banerjee and P. Mukhopadhyay (Eds.) - Phase Transformations_ Examples from Titanium and Zirconium Alloys (2007, Elsevier, Academic Press)

[15] Walter Greiner, D.A. Bromley - *Quantum Mechanics Special Chapters*, Springer (2004)

[16] EfthimiosKaxiras - *Atomic and electronic structure of solids*, Cambridge University Press (2003)

[17] David S. Sholl, Janice A. Steckel - *Density Functional Theory A Practical Introduction*, Wiley (2009)

[18] Philip L. Taylor, OlleHeinonen, *A quantum approach to condensed matter physics* Cambridge University Press, (2002)

[19] V. Antonov, B. Harmon, A. Yaresko *Electronic Structure and Magneto-Optical Properties of Solids*, Kluwer Academic Publishers, (2004)

[20] Richard M. Martin, *electronic structure basic theory and practical methods*, Cambridge University press (2004)

[21] Mark Fox, *Optical properties of solids*, Oxford University Press (2001)

[22] David A. B.Miller, Quantum Mechanics for Scientistsand Engineers, Cambridge University Press (2008)

[23] Victor Antonov,Bruce Harmon, Alexander Yaresko, *Electronic Structure and Magneto-Optical Properties Of Solids*, Kluwer Academic Publishers New York, Boston, Dordrecht, London, Moscow (2004)

[24] https://nanohub.org/resources/27109 (22 Aug 2017)

[25] P. Giannozzi *Hands-on Tutorial on Electronic Structure Computations* (2013)

[26] Algorithm PWscf User's Guide (v.6.5MaX)

[27] R. R. Pawar, and V. T. Deshpande, *Acta Crystallogr.*, 1968, 24A, 316.

[28] Heh-jeong Mo Zhang on Energy Band Structure of Ferromagnetic Nickel Louisiana State University and Agricultural & Mechanical College (1969)

[29] B. Olinger and J. C. Jamieson, *High Temp. High Pressures*, 1973, 5, 123

[30] Jiro Yamashita, Mituru Fukuchi, and Shinya Wakoh on Energy band structure of Nickel (1963)

[31] W. Borgiel & W. Nolting on the article Zeitschrift für Physik B Condensed Matter volume 78, pages241–253(1990)

[32] https://en.m.wikipedia.org/wiki/Iron (Retrived 2 Sep 2020)

[33] Jiro Yamashita, Mituru Fukuchi and Shinya Wakoh On article Energy Band Structure of Nickel J. Phys. Soc. Jpn. 18, pp. 999-1009 (1963) [11 Pages]

[34] https://en.m.wikipedia.org/wiki/Nickel(Retrived 4 Sep 2020)

[35] Tashi Nautiyal and Sushil Auluck on Journal Electronic structure of ferromagnetic iron: Band structure and optical properties Phys. Rev. B **34**, 2299 – Published 15 August 1986

[36] L.M. Sandratskii, P.G. Guletskii on article Energy band structure of BBC iron at finite temperatures(1986)

[37] **Vivek Kumr Jain, N.Lakshmi, Rakesh Jin and Aarti Rani Chandra** on Electronic Structure, Elastic, Magnetic, and Optical Properties of Fe_2MnZ (2018)

[38] Carme Rovira, Karel Kunc, Jürg Hutter, Pietro Ballone, and Michele Parrinello on Equilibrium Geometries and Electronic Structure of Iron−Porphyrin Complexes (1997)

[39] **Wigner and Seitz** band structure of Nickel(1993)

[40] C. S. Wang and J. Callaway on article Band structure of nickel: Spin-orbit coupling, the Fermi surface, and the optical conductivity Phys. Rev. B **9**, 4897 – Published 1 June 1974

[41] N.I .**Kulikov, V.N. Borzunov, and A.D. Zvonkov** on The electronic band structure and interatomic bond in nickel and titanium hydrides (1978)

[42] Algorithm PWscf User's Guide (v.6.5MaX)

[43] R. R. Pawar, and V. T. Deshpande, *Acta Crystallogr*., 1968, 24A, 316.

[44] Doru M. Stefanescus and S.Katz on Thermodynamic properties of Iron-Base Alloys (2008)

[45] Azom on Nickel(Ni) – Properties, Applicati[50]ons (2001)

[46] https://www.vector stock.com/royalty-free-vectors/lattice vectors (Retrived 10 Aug 2020)

[47] https://www.physics-in-a –nutshell.com/article /4/lattice-basis-and-crysral (Retrived 10 Aug 2020)

[48] https://www.physics-in-a –nutshell.com/article /4/cell-primitive-cell-and-winger-seitz-cell (Retrived 11 Aug 2020)

[49] https://www.Sciencedirect.com/topic/enginering/lattice-plane (Retrived 13 Aug 2020)

[50] https://en.m.wikipedia.org/wiki/miller_index (Retrived 10 Aug 2020)

[51]] https://en.m.wikipedia.org/wiki/Bravais_lattice (Retrived 10 Aug 2020)

[52] https://en.m.wikipedia.org/wiki/Brillouin zone (Retrived 10 Aug 2020)

[53] https://www.Sciencedirect.com/topic/enginering/density of states (Retrived 10 Aug 2020)

[54] www.gogle.crystal structure of cubic lattice.com Retrived 12 Aug 2020)

[55] www.gogle.typical molecular potential for the nuclei in the molecule.com (Retrived 10 Aug 2020)

[56] www.gogle.systemic representation of wave function (Retrived 10 Aug 2020)

[57] https://nanohub.org/resources/27109 (22 Aug 2017)

[58] https://periodictable.com/Elements/024/data.html (Retrived 25Aug 2020)

APPENDIX

[A]. LIST OF TABLES:

Cut-off kinetic energy and its corresponding total energy of Fe:

cut-off energy (Ry)	Total energy (Ry)
40	-254.26503904
45	-254.32064508
50	-254.33723513
55	-254.34065383
60	-254.34159182
65	-254.34300724
70	-254.34484420
75	-254.34654298
80	-254.34779072
85	-254.34848899
90	-254.34863179
95	-254.34883173
100	-254.34885412
110	-254.34901763
115	-254.34916002
120	-254.34926717

Cut-off kinetic energy and its corresponding total energy of Ni

cut-off energy (Ry)	Total energy (Ry
40	-428.63746167
45	-428.99429593
50	-429.11107644
55	-429.14241792
60	-429.14828925
65	-429.14956689
70	-429.15156048
75	-429.15456226
80	-429.15762339
85	-429.16005990
90	-429.16167985
95	-429.16259609
100	-429.16302437
105	-429.16320536
110	-429.16330685
115	-429.16341569
120	-429.16367707

Variation of total energy with k-point grid of Fe

K-point	Total energy (Ry)
2	-254.32327541
4	-254.33580763
6	-254.34767814
8	-254.34883173
10	-254.34829623
12	-254.34886663
14	-254.34893799
16	-254.34861295
18	-254.34862690

Variation of total energy with k-point grid of Ni:

K-point	Total energy (Ry)
2	-429.17649712
4	-429.16386628
6	-429.16250472
8	-429.16271115
10	-429.16265779
12	-429.16263758
14	-429.16263666
16	-429.16263752
18	-429.16263796
20	-429.16263844

Variation of total energy with lattice constant of Fe:

Lattice constant (Bohr)	Total energy (Ry)
5.02	-254.31838407
5.12	-254.33139824
5.22	-254.33912828
5.32	-254.34254759
5.42	-254.34255156
5.52	-254.33971232
5.62	-254.33462185
5.72	-254.32606852
5.82	-254.31913943
5.92	-254.31071264

Variation of total energy with lattice constant of Ni

Lattice constant (Bohr)	Total energy (Ry)
6.26	-429.13448406
6.36	-429.14406075
6.46	-429.15029904
6.56	-429.15367126
6.66	-429.15468396
6.76	-429.15366412
6.86	-429.15096893
6.96	-429.14688179
7.06	-429.14163804
7.16	-429.13546671

Variation of total energy with degauss of Fe

Degauss	Total energy (Ry)
0.01	-254.34883173
0.02	-254.34883931
0.03	-254.34874287
0.04	-254.34813266
0.05	-254.34668386
0.06	-254.34442172
0.07	-254.34174617
0.08	-254.33873066
0.09	-254.33564958
0.1	-254.33290207

The Variation of total energy with degauss of Ni

Degauss	Total energy (Ry)
0.01	-429.16253574
0.02	-429.16271115
0.03	-429.16235014
0.04	-429.16126019
0.05	-429.15963922
0.06	-429.15761303
0.07	-429.15525609
0.08	-429.15259987
0.09	-429.14965993
0.1	-429.14648094

[B]. Different input Files:

List 1: Input script for scf final

Fe

```
 &control
    Calculation = 'scf'
    Prefix='Fe',
    pseudo_dir = '/home/anup/qe-6.5/pseudo/',
    outdir='./'
 /
 &system
    ibrav=  3,
    celldm(1) =5.42,
    nat=  1,
    ntyp= 1,
    noncolin=.true.
    lspinorb=.true.
    starting_magnetization(1)=0.5,
    occupations='smearing',
    smearing='mv',
    degauss=0.02,
    ecutwfc=95.0,
    ecutrho=760.0,
    angle1(1)=90.0
```

```
   angle2(1)=0.0
   lda_plus_u=.true.
   lda_plus_u_kind=1
   Hubbard_U(1)=2.2
   Hubbard_J(1,1)=1.75
   Hubbard_J(2,1)=0.0
 /
 &electrons
   conv_thr =  1.0d-10
!    diagonalization='cg'
 /
ATOMIC_SPECIES
Fe  55.845    Fe.rel-pbe-spn-rrkjus_psl.0.2.1.UPF

ATOMIC_POSITIONS alat
Fe  0.00   0.00   0.00
K_POINTS AUTOMATTIC
8  8  8  1  1  1
```

Ni

```
&control
   calculation='scf'
   restart_mode='from_scratch',
```

```
   prefix='Ni',
   pseudo_dir =  '/home/anup/qe-6.5/pseudo',
   outdir='./'
/
&system
   ibrav=2,
   celldm(1) =6.66,
   nat=1,
   ntyp=1,
   nspin = 2,
   starting_magnetization(1)=0.7,
   ecutwfc = 95,
   ecutrho = 760,
   occupations='smearing',
   smearing='mv',
   degauss=0.02
/
&electrons
   conv_thr = 1.0e-10
   mixing_beta = 0.7
/
ATOMIC_SPECIES
 Ni 58.69    Ni.pbe-spn-kjpaw_psl.1.0.0.UPF
```

```
ATOMIC_POSITIONS alat
 Ni 0.0 0.0 0.0
K_POINTS (automatic)
6 6 6 1 1 1
```

List 2: Input script for nscf calculation of Band

Fe

```
&control
   calculation = 'nscf’
   prefix='Fe',
   pseudo_dir = '/home/anup/qe-6.5/pseudo/',
   outdir='./'
/
 &system
   ibrav=  3,
   celldm(1) =5.42,
   nat=  1,
   ntyp= 1,
   noncolin=.true.
   lspinorb=.true.
   starting_magnetization(1)=0.5,
   occupations='smearing',
   smearing='mv',
   degauss=0.02
```

```
   ecutwfc=95.0,
   ecutrho=760.0,
   angle1(1)=90.0
   angle2(1)=0.0
   lda_plus_u=.true.
   lda_plus_u_kind=1
   Hubbard_U(1)=2.2
   Hubbard_J(1,1)=1.75
   Hubbard_J(2,1)=0.0
 /
 &electrons
   conv_thr =  1.0d-10
!    diagonalization='cg'
 /
ATOMIC_SPECIES
Fe  55.845    Fe.rel-pbe-spn-rrkjus_psl.0.2.1.UPF

ATOMIC_POSITIONS alat
Fe  0.00   0.00   0.00
K_POINTS AUTOMATTIC
12  12  12  0  0  0
```

Ni

```
&control
   calculation='nscf'
   restart_mode='from_scratch',
   prefix='Ni',
   pseudo_dir =  '/home/anup/qe-6.5/pseudo',
   outdir='./'
/
 &system
   ibrav=2,
   celldm(1) =6.66,
   nat=1,
   ntyp=1,
   nspin = 2,
   starting_magnetization(1)=0.7,
   ecutwfc = 95,
   ecutrho = 760,
   occupations='smearing',
   smearing='mv',
   degauss=0.02
/
 &electrons
   conv_thr = 1.0e-10
   mixing_beta = 0.7
```

/

ATOMIC_SPECIES

Ni 58.69 Ni.pbe-spn-kjpaw_psl.1.0.0.UPF

ATOMIC_POSITIONS alat

Ni 0.0 0.0 0.0

K_POINTS (automatic)

10 10 10 0 0 0

List 3: Input script for Bands.in

Fe

&bands

prefix ='Fe'

outdir ='./'

filband ='Fe.bands.dat'

lsym =.true.,

/

Ni

&bands

prefix ='Ni'

outdir ='./'

filband ='Ni.bands.dat'

lsym =.true.,

/

List 4: Input script for DOS.in

Fe

```
&dos
   prefix='Fe'
   outdir='./'
   ngauss=-1
   degauss=0.02
   DeltaE=0.01
   fildos='Fe.dos.dat'
/
```

Ni

```
&dos
   prefix='Ni'
   outdir='./'
   ngauss=-1
   degauss=0.02
   DeltaE=0.01
   fildos='Ni.dos.dat'
/
```

List 5: Input script for PDOS.in

Fe

```
&projwfc
   prefix='Fe'
   outdir='./'
   ngauss=-1
   degauss=0.02
   DeltaE=0.01
   filpdos='Fe.pdos.dat'
/
```

Ni

```
&projwfc
   prefix='Ni'
   outdir='./'
   ngauss=-1
   degauss=0.02
   DeltaE=0.01
   filpdos='Ni.pdos.dat'
/
```

List 7: Input script for dos plot

Fe

```
set term postscript enhanced color 'Helvetica-Bold' 20

set output 'Fe.dos.ps'

set autoscale

unset log

unset label

set xtic -10,1

set ytic 0,0.5

set xlabel "E-Ef (ev)"

set ylabel "Dos"

#set key 0.01,100

set xr [-9:6]

#set yr [0:325]

ef=17.8639

plot "Fe.dos.dat" using ($1-ef):2 title 'Dos of Fe'  w l lw 5 lt 5 lc rgb "red"

set output

! ps2pdf Fe.dos.ps

! rm Fe.dos.ps

pause -1 "Hit any key to continue\n"
```

Ni

```
set term postscript enhanced color 'Helvetica-Bold' 20

set output 'Ni.dos.ps'
```

```
set autoscale

unset log

unset label

set xtic -10,1

set ytic 0,0.5

set xlabel "E-Ef (ev)"

set ylabel "Dos"

#set key 0.01,100

set xr [-9:6]

#set yr [0:325]

ef=17.8637

plot "Ni.dos.dat" using ($1-ef):2 title 'Dos of Ni'  w l lw 5 lt 5 lc rgb "red"

set output

! ps2pdf Ni.dos.ps

! rm Ni.dos.ps

pause -1 "Hit any key to continue\n"
```

List 7: Input script for bands plot

Fe

```
set terminal postscript enhanced color "Helvetica" 20

set output "Fe.band.ps"

set autoscale

unset xtics

set ytics -6,1

set bmargin 3

set xlabel "kpaths" offset 0,-1,0

set ylabel "E-Ef (eV)"

set label "{/Symbol G}" at -0.02,-6.4

set label "{/Symbol G}" at 2.39559,-6.4

set label "H" at 0.98094,-6.4

set label "N" at 1.68536,-6.4

set label "P" at 3.26301,-6.4

set arrow from 1.00405, graph 0 to 1.00405, graph 1 nohead

set arrow from 1.70960, graph 0 to 1.70960, graph 1 nohead

set arrow from 2.41414, graph 0 to 2.41414, graph 1 nohead

set arrow from 3.28954, graph 0 to 3.28954, graph 1 nohead

#set key 0.01,100

set xr [0.0:3.29154]

set yr [-6:8]

ef=17.5446
```

```
plot "Fe.bands.dat.gnu" using 1:($2-ef) title 'bands of Fe' w l lw 3 lt 4 lc rgb "black"
set output
! ps2pdf Fe.band.ps
! rm Fe.band.ps
pause -1 "Hit any key to continue\n"
```

Ni

```
set terminal postscript enhanced color "Helvetica" 20
set output "Ni.band.ps"
set autoscale
unset log
set xzeroaxis lw 1 lc -1
unset xtics
set ytics -10,4
set bmargin 3
set xlabel "k-paths" offset 0,-1,0
set ylabel "E-Ef (eV)"
set label "{/symbol G}" at 0.00000,-10.75
set label "{/symbol G}" at 5.534831,-10.75
set label "X" at 0.945531, -10.75
set label "W" at 2.40989,  -10.75
set label "K" at 4.39793,  -10.75
set label "L" at 6.23081,  -10.75
set label "U" at 6.79328,  -10.75
```

```
set label "W" at 8.34492,  -10.75

set label "L" at 9.39694,  -10.75

set arrow from 0.00000,  graph 0 to 0.00000,  graph 1 nohead

set arrow from 5.534831, graph 0 to 5.534831, graph 1 nohead

set arrow from 0.945531, graph 0 to 0.945531, graph 1 nohead

set arrow from 2.40989,  graph 0 to 2.40989,  graph 1 nohead

set arrow from 4.39793,  graph 0 to 4.39793,  graph 1 nohead

set arrow from 6.23081,  graph 0 to 6.23081,  graph 1 nohead

set arrow from 6.79328,  graph 0 to 6.79328,  graph 1 nohead

set arrow from 8.34492,  graph 0 to 8.34492,  graph 1 nohead

set arrow from 9.39694,  graph 0 to 9.39694,  graph 1 nohead

#set key 0.01,100

set xr [0:10]

set yr [-10:30]

ef=17.8637

plot "Ni.bands.dat.gnu" using 1:($2-ef) title 'bands of Ni' w l lw 3 lt 4 lc rgb
"blue"

set output

! ps2pdf Ni.band.ps

! rm Ni.band.ps

pause -1 "Hit any key to continue\n"
```

List 8: Input script for plot pdos

Fe

```
set term postscript enhanced color 'Helvetica-Bold' 20

set output 'Fe.pdos.ps'

set autoscale

unset log

unset label

set xtic auto

set ytic 0,0.8

set xlabel "Energy (ev)"

set ylabel "pdos"

set xr [10:22]

set arrow from 17.5446,0.0 to 17.5446,4.8, 2 nohead ls 10 dt 2

plot  "atom_Fe_s.dat" using 1:2 title 'Fe s orbital' w l lw 3 lt 1 lc rgb "red",\

     "atom_Fe_p.dat" using 1:2 title 'Fe p orbital' w l lw 3 lt 1 lc rgb "blue",\

     "atom_Fe_d.dat" using 1:2 title 'Fe d orbital' w l lw 3 lt 1 lc rgb "green",\

     "atom_Fe_tot.dat" using 1:2 title 'Fe total' w l lw 3 lt 1 lc rgb "yellow",\


set output

 ! ps2pdf Fe.pdos.ps

 ! rm Fe.pdos.ps

pause -1 "hit any key to continue\n"
```

Ni

```
set term postscript enhanced color 'Helvetica-Bold' 20
set output 'Ni.pdos.ps'
set autoscale
unset log
unset label
set xtic 10,2
set ytic auto
set xlabel "Energy (ev)"
set ylabel "Pdos"
set xr [10:20]
set yr [0:3]
set arrow from  17.8601,0.0 to  17.8601,3, 2 nohead ls 10 dt 2
plot  "atom_Ni_s.dat" using 1:2 title 'Ni s orbital' w l lw 3 lt 1 lc rgb "blue",\
     "atom_Ni_p.dat" using 1:2 title 'Ni p orbital' w l lw 3 lt 1 lc rgb "red",\
     "atom_Ni_d.dat" using 1:2 title 'Ni d orbital' w l lw 3 lt 1 lc rgb "green",\
     "atom_Ni_tot.dat" using 1:2 title 'Ni total orbital' w l lw 3 lt 1 lc rgb "yellow",
set output
 ! ps2pdf Ni.pdos.ps
 ! rm Ni.pdos.ps
pause -1 "hit any key to continue\n"
```